Biol. Pharm. Bull. **28**(10) 1934—1938 (2005) Vol. 28, No. 10

Pharmacokinetic Characteristics of Amiodarone in Long-Term Oral Therapy in Japanese Population

Asami KASHIMA,[a] Miho FUNAHASHI,[a] Kyoko FUKUMOTO,[a] Kazuo KOMAMURA,[b] Shiro KAMAKURA,[c] Masafumi KITAKAZE,[c] and Kazuyuki UENO*,[a]

[a] *Department of Pharmaceutical Sciences, Niigata University of Pharmacy and Applied Life Sciences; 5–13–2 Kamishin'ei-cho, Niigata 950–2081, Japan:* [b] *Department of Research, National Cardiovascular Center; and* [c] *Department of Cardiology, National Cardiovascular Center; 5–7–1 Fujishirodai, Suita, Osaka 565–8565, Japan.*

Received March 29, 2005; accepted June 9, 2005

To evaluate the pharmacokinetic properties and an optimum dose schedule of amiodarone in long-term oral therapy, serum concentrations of amiodarone and its metabolite, desethylamiodarone, were monitored from 345 Japanese inpatients who received amiodarone therapy for a variety of cardiac arrhythmias. Serum amiodarone and desethylamiodarone concentrations were determined by high performance liquid chromatography system. It was observed that the amiodarone and desethylamiodarone concentrations gradually increased with time. The frequency distribution in the amiodarone clearance of 245 subjects, who received fixed maintenance amiodarone therapy for at least 6 months, was nearly a unimodal one. The variation in the ratio of desetylamiodarone to amiodarone concentration in serum was very small. Although no differences in age, dose, dose duration, amiodarone or desethyamiodarone concentration or ratio were observed between men and women: however, the mean amiodarone clearance of women was significantly higer than that of men. The laboratory data were mostly within normal values and no significant relations were observed between serum amiodarone concentration and clinical laboratory data. These results suggest that the individual variation in pharmacokinetics of amiodarone is comparatively small, which might be sufficient to decide that the maintenance dose was the same one (200 mg/d) in long-term oral amiodarone therapy.

Key words amiodarone; long-term therapy; pharmacokinetics; Japanese

Amiodarone is an important antiarrhythmic agent in the prevention of sustained ventricular tachycardia and fibrillation. Until recently, however, concerns about potentially dangerous non-cardiac side effects and its complex pharmacokinetics have limited the use of amiodarone to the most drug-resistant and high risk subjects. Nonetheless, amiodarone appears to significantly improve in patients after myocardial infarction, and amiodarone has begun to be accepted as a first-line therapy as opposed to a last-chance drug. Amiodarone's increase in popularity is exhibited by its rapidly growing use in the management of refractory atrial arrhythmias.[1,2]

On the other hand, amiodarone is predominantly metabolized to desethylamiodarone, which is the active metabolite, by cytochrome P450(CYP)3A4 and CYP2C8, and desethylamiodarone is further metabolized by CYP3A4.[3,4] It has unique pharmacokinetic properties, with 55 d constituting a typical half-life, and pharmacokinetic interactions with various therapeutic agents,[5—7] including warfarin,[8—10] phenytoin,[11—13] flecainide[14—16] and cyclosporine.[17,18] With the growing number of patients maintained on long-term amiodarone therapy, it is more important to evaluate interindividual variability and characteristics in detail; however, few reports of the pharmacokinetics of amiodarone in long-term therapy have been published,[19] especially, no report was published using the Japanese population.

The aim of this study was to evaluate an optimum dose schedule and pharmacokinetic properties of amiodarone in long-term oral therapy in the Japanese population.

Subjects Data were collected from 345 Japanese inpatients who received amiodarone therapy for a variety of cardiac arrhythmias at the National Cardiovascular Center between September 1998 and December 2003. Patients received loading doses from 200 to 400 mg/d for 2 weeks (bid, 0700 and 1900 h), as determined by their cardiologist on the clinical response, without attempts to achieve a specific serum concentration, and received daily maintenance doses from 100 to 200 mg (bid, 0700 and 1900 h). The most common long-term maintenance dose was 200 mg/d. Because all subjects were inpatients, compliance was ensured through administration by a nurse or pharmacist.

Blood Sampling To determine the serum concentration of amiodarone and desethylamiodarone and laboratory examination data, blood samples were drawn at 0700 h from an arm vein. Blood samples were centrifuged at 3000 rpm for 10 min, and serum samples were obtained. Written informed consent was obtained from all subjects before participation in this study.

Assay Serum amiodarone and desethylamiodarone were determined by an HPLC system using amitriptyline as an internal standard (IS).[20] In brief, amiodarone and desethylamiodarone were extracted with diethylether followed by evaporation. The residue was reconstituted in methanol before injection into the HPLC system. The HPLC system consisted of a reverse-phase column (Shim-pack, CLC-ODS, Shimadzu Corp., Kyoto, Japan), and an ultraviolet absorbance detector operated at 242 nm. The mobile phase consisted of a mixture of methanol, water, and 28% ammonia water (91 : 8.8 : 0.2 by volume), and the flow rate was 1.5 ml/min. Retention times of the IS, desethylamiodarone and amiodarone were 6.6, 11.7, and 19.2 min, respectively. The minimum measurable concentration was 50 ng/ml when 0.5 ml of serum was used. Inter- and intraday variations were less than 5.0%.

Pharmacokinetic Analysis It is well known that amiodarone has a long half-life as does desethylamiodarone, which is an inhibitor of metabolism of amiodarone through

* To whom correspondence should be addressed. e-mail: uenok@niigata-pharm.ac.jp

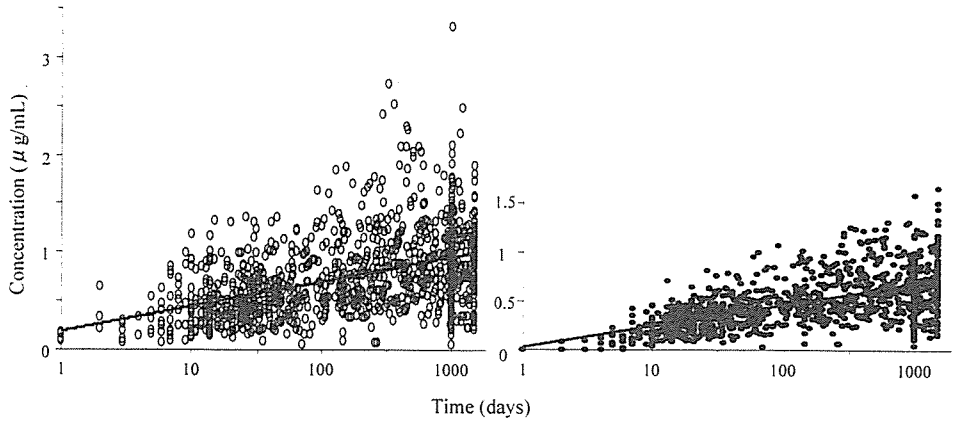

Fig. 1. Distribution of 1031 Amiodarone and Desethylamiodarone Concentrations *versus* Time Observations Collected from 345 Inpatients Monitored for a Mean of 446 d

Right panel indicate amiodarone and at left is desethylamiodarone. The regression equation was determined by a least-squares method, $y=0.0296+0.216 \log x$, $r^2=0.357$ (amiodarone) and $y=0.187+0.256 \log x$, $r^2=0.212$ (desethylamiodarone), as shown with the solid line.

CYP3A4. Therefore, the time required to reach a steady state of amiodarone concentration in serum is extraordinarily long. Thus, because blood samples were collected from inpatients who were administered fixed-maintenance dose of amiodarone for at least 180 d after the loading dose for 2 weeks. It was assumed that their serum amiodarone concentrations had reached a steady state. All samples were taken at the same time, 0700 h (12 h after the administration of amiodarone). Therefore, we used C_{0700} instead of C_{mean} (mean concentration); as a result, the oral clearance of amiodarone (CL/F) was calculated according to the following equations:

$$CL/F=(\text{Dose}/\text{BW}/t)/C_{0700}$$

$$CL(\text{BMI})/F=(\text{Dose}/\text{BMI-BW}/t)/C_{0700}$$

$$CL(\text{BSA})/F=(\text{Dose}/\text{BW}/t)/C_{0700}$$

Where Dose is the daily dose of amiodarone, BW is the body weight, BMI-BW is BW corrected by body mass index (BMI) (BW×(22.0/BMI)), BSA is the body surface area, F is bioavailability, t is the dose interval, and C_{0700} is the serum concentration of amiodarone at 0700 h.

Statistical Analysis The data are expressed as mean± standard deviation (S.D.). Statistical analysis was performed with the use of the unpaired Student's t-test. The criterion of significance was $p<0.05$.

RESULTS

The demographic characteristics of this study population are listed in Table 1. Figure 1 shows the distribution since the beginning to 1500 d after the therapy using serum 1031 amiodarone and desethylamiodarone concentrations *versus* time observations collected from 345 inpatients (men 274, women 71). The duration of dosing was fixed at 1500 d in the subjects whose observation time exceed 1500 d. It was observed that the amiodarone and desethylamiodarone concentrations gradually increased with time, whereas desethylamiodarone concentrations were below the limit of this measurement in the first and second day after the start of the therapy. Comparison between serum amiodarone and desethylamiodarone concentrations per dose and the duration of dosing is listed in Table 2. Although the ratio of the desethylamiodarone concentration to the amiodarone one was nearly equal among the all durations, the amiodarone and desethylamiodarone concentration per dose gradually increased with the period of the duration.

Table 1. Demographic Characteristics of the Study Population

n	345
Age (year)	57.0±14.0
Weight (kg)	57.7±11.4
Height (cm)	164±8.6
BSA (m^2)	1.61±0.18
Dose (mg/d)	159±56.2
Duration (d)	563±526

BSA, body surface area; Duration, duration of the therapy in days to the last data employ in each patient, and duration was fixed 1500 d in patient who received amiodarone therapy for more than 1500 d. Data are presented as mean±S.D.

Table 2. Comparison between Concentrations of Amiodarone and Desethylamiodarone in Serum, and Duration of Dosing

Duration (month)	n	AMD/D	DEA/D	DEA/AMD ratio
1—2	92	0.189±0.076	0.132±0.046	0.730±0.147
2—3	42	0.209±0.097	0.140±0.050	0.720±0.173
3—4	33	0.238±0.120	0.154±0.069	0.698±0.196
4—6	45	0.274±0.114	0.194±0.075	0.737±0.161
6—12	75	0.310±0.172	0.216±0.111	0.732±0.144
12—24	73	0.345±0.158	0.242±0.099	0.749±0.150
24—	137	0.336±0.162	0.243±0.100	0.749±0.142

AMD/D and DEA/D, serum amiodarone (desethylamiodarone) concentration/daily dose of amiodarone/body weight; DEA/AMD ratio, the ratio of serum desethylamiodarone concentration/serum amiodarone concentration. Data are presented as mean± S.D.

Comparison of pharmacokinetic parameters of amiodarone between men and women who received a fix maintenance amiodarone therapy for at least six months was shown in Table 3. Although significant differences were not observed in the dose, duration, amiodarone and desethylamiodarone concentrations, or the ratio between men and women, it was observed that the CL/F, $CL(\text{BMI})/F$ and $CL(\text{BSA})/F$ of women were significantly higher than that in men, respectively. The frequency of distribution in CL/F of 245 subjects who received a fix maintenance amiodarone therapy for at

Table 3. Comparison of Demographic and Pharmacokinetic Parameters of Amiodarone between Men and Women

	Men	Women	
n	194	51	
Age (year)	54.7±14.5	53.6±15.6	NS
Weight (kg)	61.2±10.1	47.9±8.69	<0.001
Height (cm)	167±6.8	153±5.7	<0.001
BSA (m^2)	1.67±0.15	1.42±0.12	<0.001
Dose (mg/d)	157±47.0	150±51.0	NS
Duration (d)	811±445	756±403	NS
AMD Conc (μg/ml)	0.853±0.369	0.818±0.346	NS
DEA Conc (μg/ml)	0.603±0.225	0.611±0.266	NS
Ratio (DEA/AMD)	0.740±0.143	0.759±0.157	NS
CL/F (l/h/kg)	0.143±0.059	0.177±0.070	<0.001
CL(BMI)/*F*	0.149±0.711	0.203±0.113	<0.001
CL(BSA)/*F*	5.16±2.05	5.85±2.05	0.035

BSA, body surface area; Dose, daily dose of amiodarone; AMD Conc, serum amiodarone concentration; DEA Conc, serum desethylamiodarone concentration; Ratio, ratio of desethylamiodarone to amiodarone concentration in serum; *CL*, amiodarone clearance; *F*, bioavailability; *CL*(BMI), amiodarone clearance per body weight corrected by body mass index; *CL*(BAS), amiodarone clearance per BSA. Data are presented as mean±S.D.

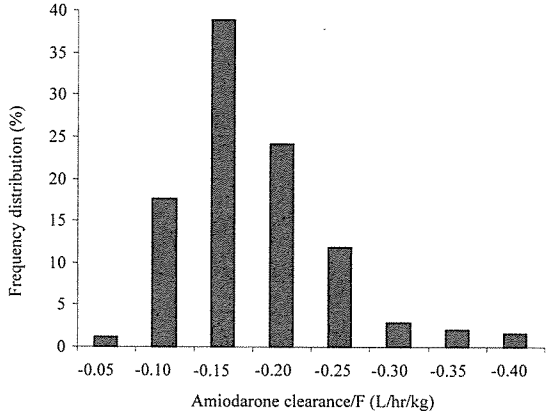

Fig. 2. Frequency Distribution of Amiodarone Clearance/*F* in 245 Japanese Subjects Who Received Fixed Maintenance Amiodarone Therapy for at Least 6 Months

F is bioavailability.

least six months is shown in Fig. 2. The relationships between age and *CL/F*, between creatinine clearance and *CL/F* and between blood urea nitrogen (BUN) are shown in Figs. 3—5. It was observed that age, creatinine clearance and BUN did not affect *CL/F*.

The relationships between serum amiodarone concentrations and clinical laboratory data are shown in Fig. 6. No significant relations were observed between serum amiodarone concentrations and clinical data.

DISCUSSION

As shown in Fig. 1, it was observed that serum amiodarone and desethylamiodarone concentrations gradually increased with time, and the increase was continued for an extremely long term. It was reported that amiodarone had an extraordinarily long half-life, with 55 d constituting a typical half-life.[3] The result of this study was the same as in previous reports.[3,19] Desethylamiodarone inhibits various CYP subfamilies and transporters, including CYP3A4 and P-glycoprotein.[7,21] Amiodarone is a substrate of CYP3A4 and P-

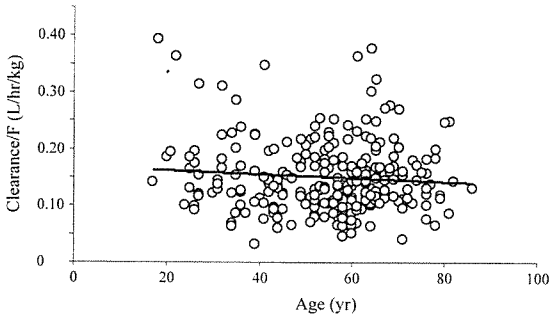

Fig. 3. Relationship between Age and Amiodarone Clearance/*F*

The regression equation determined by a least-squares method, $y=0.169+3.36\times10^{-4}x$, $r^2=0.0061$, as shown with the solid line. *F* is bioavailability.

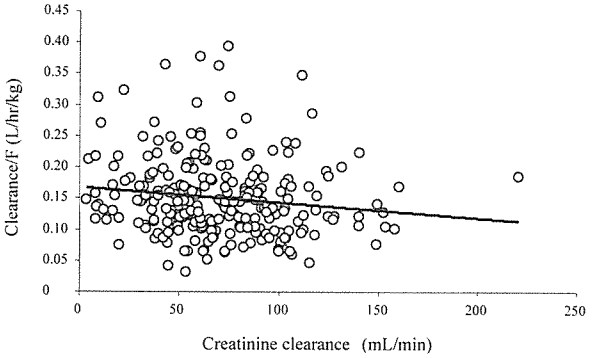

Fig. 4. Relationship between Creatinine Clearance and Amiodarone Clearance/*F*

The regression equation determined by a least-squares method, $y=0.168+2.48\times10^{-4}x$, $r^2=0.0177$, as shown with the solid line. *F* is bioavailability.

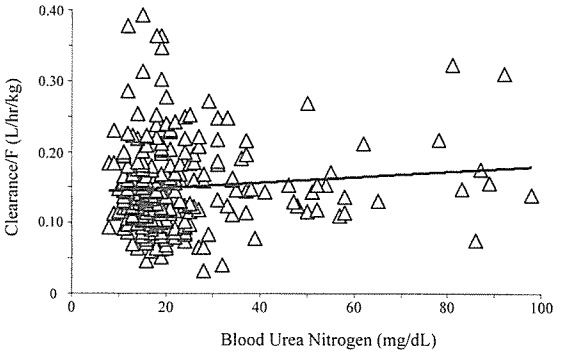

Fig. 5. Relationship between Blood Urea Nitrogen and Amiodarone Clearance /*F*

The regression equation determined by a least-squares method, $y=0.141+10^{-4}x$, $r^2=0.00932$, as shown with the solid line. *F* is bioavailability.

glycoprotein. These reports suggest the metabolite of amiodarone inhibits the metabolism and transport of the parent compound. Therefore, it is difficult to calculate the time to a reach at steady state of serum amiodarone concentration. However, as shown in Table 2, although serum amiodarone and desethylamiodarone concentrations per dose were increased with time, no difference in those concentrations per dose was observed between the duration from 12 to 24 months, and that of after 24 months, and no remarkable difference was observed in a period of over 6 months. Therefore, to evaluate the pharmacokinetics of amiodarone in long-term oral therapy, we employed the data of subjects who

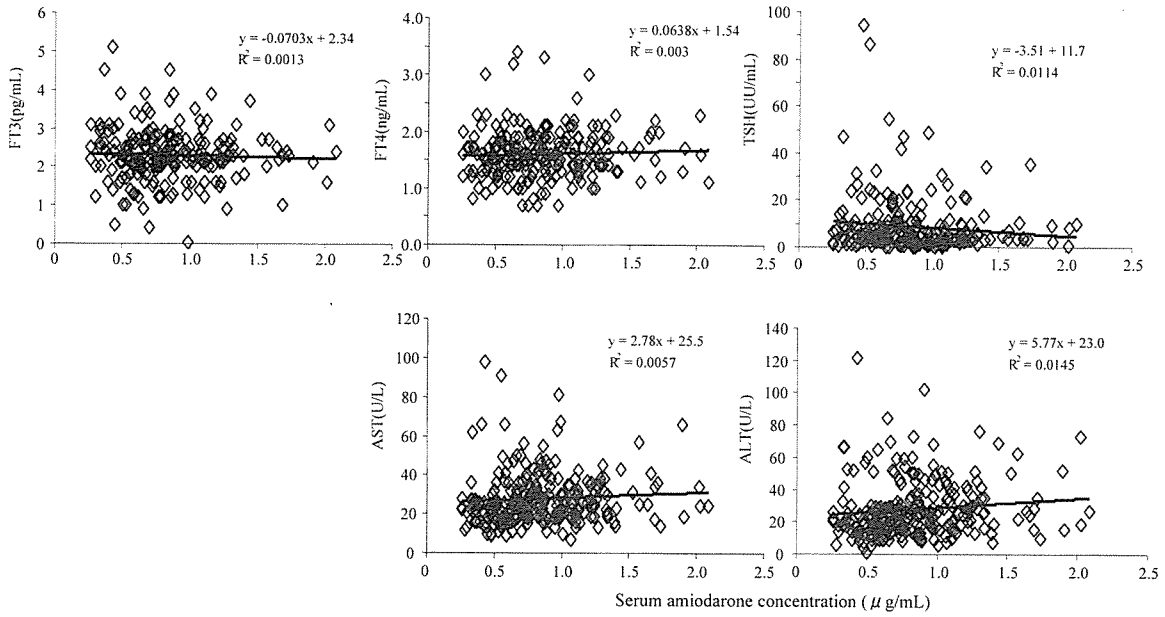

Fig. 6. Relationship between Serum Amiodarone Concentrations and Clinical Data

AST, asparatate transaminase; ALT, alanin transaminase; FT3, free triiodothyronine; FT4, free thyroxine; TSH, thyroid-stimulating hormone.

received the therapy for more than 180 d (Table 3).

As shown in Fig. 2, the frequency distribution was nearly unimodal, 13.1% of the distribution was less than mean minus 1SD, and no subjects were observed at less than mean minus 2SD. Fourteen point seven percentage of the distribution was more than mean plus 1SD, and 4.9% was more than mean plus 2SD. Variation in the ratio of the desethylamiodarone to amiodarone concentration in serum was very small. These data suggest that inter individual variation in the clearance in subjects who received a long-term maintenance fixed dose of amiodarone is comparatively small. Amiodarone is mainly metabolized to desethylamiodarone by CYP3A4 and CYP2C8, desethylamiodarone is further metabolized by CYP3A4, and amiodarone is transported by P-glycoprotein. Various CYP2D6 alleles carrying a point mutation or a combination of mutations on the chromosome have been reported, and there were poor metabolizers for CYP2D6 mediated drugs.[21,22] It was reported that there were CYP3A4 gene and MDR1 mutations. However, a remarkable difference in phenotype of CYP3A4 and P-glycoprotein mediated drugs was not observed compared with that in the phenotype of CYP2D6 mediated drugs. It is well known that the activities of CYP3A4 and P-glycoprotein contribute to the bioavailability of drugs, and the bioavailability of amiodarone is low. On the other hand, desethylamiodarone inhibits the activities of both CYP3A4 and P-glycoprotein[7,23] thus it is suggested that the bioavailability of amiodarone is gradually increased with time in subjects receiving long-term amiodarone therapy, and individual variation of the clearance decreases in subjects receiving long-term amiodarone therapy.

As shown in Table 3, no differences in age, dose, dose duration, amiodarone or desethylamiodarone concentrations, or ratio were observed between men and women; however, the mean *CL/F*, *CL*(BMI)/*F* and *CL*(BSA) of women were significantly increased compared with those of men, respectively. Hunt *et al.* found a 24% higher CYP3A4 activity in female liver microsomes than in male liver microsomes.[24] However, studies by Schmucker *et al.*,[25] Shimada *et al.*,[26] and George *et al.*,[27] which examined CYP3A4 protein content and function from human livers, were not able to show any significant sex-related differences. One proposed explanation for the differences observed in women is the presence of the female sex steroids estrogen and progesterone, which are known substrates of CYP3A4.[28,29] In this study, all subjects were elderly. Therefore, it is suggested that the sex-related difference in amiodarone clearance could not be the explanatory link. The distribution volume of amiodarone is extraordinarily large; especially, the distribution to fatty tissue is large due to the extreme affinity of amiodarone for lipids. It was reported that the body fat in women (mean age 72 years) was significantly higher than that of men (mean age 75 years).[30] Therefore, it is suggested that the difference in *CL/F* between men and women is caused by the distribution to fatty tissue. As shown in Figs. 3—5, it was observed that *CL/F* was not affected by age, creatinine clearance or BUN. Therefore, it is unnecessary to consider age or renal function for an optimum dose schedule in amiodarone therapy.

It is well known that amiodarone has potentially dangerous non-cardiac side-effects, and some of the side-effects are dose dependent.[31,32] As shown in Fig. 6, these laboratory data were mostly within the normal value, and no significant relations were observed between serum amiodarone concentrations and clinical laboratory data. Previous reports, used a small number of subjects and the dose was comparatively high. In this study, a total of 345 subjects was used and the most common maintenance dose was 200 mg/d. Therefore, it was suggested that thyroid hormone metabolism and an elevation of aminotaransferases was not affected by the amiodarone concentrations in low-dose amiodarone therapy in such a study.

In conclusion, individual variation in the pharmacokinetics of amiodarone was comparatively small, which might be sufficient to conclude that the maintenance dose is the same (200 mg/d) as in long-term oral amiodarone therapy.

REFERENCES

1) Singh B. N., *Clin. Cardiol.*, **20**, 608—618 (1997).
2) Estes N. A., Weinstock J., Wang P. J., Homoud M. K., Link M. S., *Am. J. Cardiol.*, **91**, 45D—52D (2003).
3) Latini R., Tognoni G., Kates R. E., *Clin. Pharmacokinet.*, **9**, 136—156 (1984).
4) Ohyama K., Nakajima M., Nakamura S., Shimada N., Yamazaki H., Yokoi T., *Drug Metab. Dispos.*, **28**, 1303—1310 (2000).
5) Lesko L. J., *Clin. Pharmacokinet.*, **17**, 130—140 (1989).
6) Marcus F. I., *Am. Heart J.*, **106**, 924—930 (1983).
7) Ohyama K., Nakajima M., Suzuki M., Shimada N., Yamazaki H., Yokoi T., *Br. J. Clin. Pharmacol.*, **49**, 244—253 (2000).
8) Heimark L. D., Wienkers L., Kunze K., Gibaldi M., Eddy A. C., Trager W. F., Robert A. O'R., Darklis A. G., *Clin. Pharmacol. Ther.*, **51**, 398—407 (1992).
9) Watt A. H., Stephens M. R., Buss D. C., Routledge P. A., *Br. J. Clin. Pharmacol.*, **20**, 707—709 (1985).
10) Almog S., Shafran N., Halkin H., Weiss P., Farfel Z., Martinowitz U., Bank H., *Eur. J. Clin. Pharmacol.*, **28**, 257—261 (1985).
11) Nolan P. E., Jr., Marcus F. I., Karol M. D., Hoyer G. L., Gear K., *J. Clin. Pharmacol.*, **30**, 1112—1119 (1990).
12) Nolan P. E., Jr., Erstad B. L., Hoyer G. L., Bliss M., Gear K., Marcus F. I., *Am. J. Cardiol.*, **65**, 1252—1257 (1990).
13) Nolan P. E., Jr., Marcus F. I., Hoyer G. L., Bliss M., Gear K., *Clin. Pharmacol. Ther.*, **46**, 43—50 (1989).
14) Shea P., Lal R., Kim S. S., Schechtman K., Ruffy R., *J. Am. Coll. Cardiol.*, **7**, 1127—1130 (1986).
15) Haefeli W. E., Bargetzi M. J., Follath F., Meyer U. A., *J. Cardiovasc. Pharmacol.*, **15**, 776—779 (1990).
16) Funck-Brentano C., Becquemont L., Kroemer H. K., Buhl K., Knebel N. G., Eichelbaum M., Jaillon P., *Clin. Pharmacol. Ther.*, **55**, 256—269 (1994).
17) Nicolau D. P., Uber W. E., Crumbley A. J., Strange C., *J. Heart Lung Transplant.*, **11**, 564—568 (1992).
18) Chitwood K. K., Abdul-Haqq A. J., Heim-Duthoy K. L., *Ann. Pharmacother.*, **27**, 569—571 (1993).
19) Pollak P. T., Bouillon T., Shafer S. L., *Clin. Pharmacol. Ther.*, **67**, 642—652 (2000).
20) Masaki K., Ueno K., Tsuji M., Hiraki K., Kamakura S., Takada M., Shibakawa M., *Jpn. J. Hosp. Pharm.*, **25**, 28—33 (1999).
21) Eichelbaum M., Gross A. S., *Pharmacol. Ther.*, **46**, 377—394 (1990).
22) Kubota T., Yamamura Y., Ohkawa N., Hara H., Chiba K., *Br. J. Clin. Phramacol.*, **50**, 31—34 (2000).
23) Kakumoto M., Takara K., Sakaeda T., Tanigawara Y., Kita T., Okumura K., *Biol. Pharm. Bull.*, **25**, 1604—1607 (2002).
24) Hunt C. M., Westerkam W. R., Stave G. M., *Biochem. Pharmacol.*, **44**, 275—283 (1992).
25) Schmucker D. L., Woodhouse K. W., Wang R. K., Wynne H., James O. F., McManus M., *Clin. Pharmacol. Ther.*, **48**, 365—374 (1990).
26) Shimada T., Yamazaki H., Mimura M., Inui Y., *J. Pharmacol. Exp. Ther.*, **270**, 414—423 (1994).
27) George J., Byth K., Farrell G. C., *Biochem. Pharmacol.*, **50**, 727—730 (1995).
28) Palovaara S., Kivisto K. T., Tapanainen P., Manninen P., Neuvonen P. J., Laine K., *Br. J. Clin. Pharmacol.*, **50**, 333—337 (2000).
29) Williams P. A., Cosme J., Vinkovic D. M., Ward A., Angove H. C., Day P. J., Vonrhein C., Tickle I. J., Jhoti H., *Science*, **300**, 683—686 (2004).
30) Fukagawa N. K., Bandini L. G., Young J. B., *Am. J. Physiol.*, **259**, 233—238 (1990).
31) Staubli M., Bircher J., Galeazzi R. L., Remund H., Studer H., *Eur. J. Clin. Pharmacol.*, **24**, 485—494 (1983).
32) Heger J. J., Prystowsky E. N., Zipes D. P., *Am. Heart J.*, **16**, 931—935 (1983).

nature genetics

Lamr1 functional retroposon causes right ventricular dysplasia in mice

Yoshihiro Asano[1], Seiji Takashima[1], Masanori Asakura[1], Yasunori Shintani[1], Yulin Liao[1], Tetsuo Minamino[1], Hiroshi Asanuma[1], Shoji Sanada[1], Jiyoong Kim[2], Akiko Ogai[2], Tomi Fukushima[1], Yumiko Oikawa[1], Yasushi Okazaki[3], Yasufumi Kaneda[4], Manabu Sato[4], Jun-ichi Miyazaki[5], Soichiro Kitamura[2], Hitonobu Tomoike[2], Masafumi Kitakaze[2] & Masatsugu Hori[1]

Arrhythmogenic right ventricular dysplasia (ARVD) is a hereditary cardiomyopathy that causes sudden death in the young. We found a line of mice with inherited right ventricular dysplasia (RVD) caused by a mutation of the gene laminin receptor 1 (*Lamr1*). This locus contained an intron-processed retroposon that was transcribed in the mice with RVD. Introduction of a mutated *Lamr1* gene into normal mice by breeding or by direct injection caused susceptibility to RVD, which was similar to that seen in the RVD mice. An *in vitro* study of cardiomyocytes expressing the product of mutated *Lamr1* showed early cell death accompanied by alteration of the chromatin architecture. We found that heterochromatin protein 1 (HP1) bound specifically to mutant LAMR1. HP1 is a dynamic regulator of heterochromatin sites, suggesting that mutant LAMR1 impairs a crucial process of transcriptional regulation. Indeed, mutant LAMR1 caused specific changes to gene expression in cardiomyocytes, as detected by gene chip analysis. Thus, we concluded that products of the *Lamr1* retroposon interact with HP1 to cause degeneration of cardiomyocytes. This mechanism may also contribute to the etiology of human ARVD.

ARVD is a type of right ventricular cardiomyopathy characterized by the gradual loss of cardiomyocytes and compensatory replacement with either adipose or fibrous tissue. ARVD is a primary cause of sudden cardiac death in juveniles and athletes, but is difficult to diagnose before the onset of cardiac events. In Italy, ARVD accounts for 20% of all sudden deaths in individuals under 35 years old and 22% of sudden deaths in athletes[1]. The etiology of this disease is still unknown. Familial occurrence is reported in about 30% of individuals with ARVD. Six associated loci have been mapped: ARVD1, 14q23 (ref. 1); ARVD2, 1q42 (ref. 1); ARVD3, 14q12 (ref. 2); ARVD4, 2q32 (ref. 3); ARVD5, 3p23 (ref. 4); and ARVD6, 10p12 (ref. 5). The only gene identified so far is that underlying ARVD2, which corresponds to the cardiac ryanodine receptor gene and causes a condition with different features from those of the other forms of ARVD[6]. As in humans, a naturally occurring phenotype of RVD has been reported in dogs, cats and minks[7–10], but the genes responsible have not been identified.

We report here a new mouse model of ARVD: we identified a retroposon insertion encoding a mutant form of the nuclear protein laminin receptor 1 (LAMR1) by positional cloning. LAMR1 is one of the ribosomal proteins localized in the nucleus and involved in apoptosis[11,12]. We also report possible molecular mechanisms leading to ARVD.

RESULTS

Mouse model of ARVD

We found a mouse model of ARVD by chance during the screening of antidiabetic compounds with KK obese mice that were originally isolated on the basis of hyperglycemia[13,14]. The mouse strain, named KK/Rvd, developed severe RVD. Macroscopic examination of the heart of these mice at 8 weeks of age showed massive fibrosis of the entire right ventricular wall that never extended to the left ventricle (**Fig. 1a,b**). This resembles the histopathology of human ARVD. We found that the outer third of the right ventricular wall was replaced by fibrous tissue and that calcification also occurred (**Fig. 1c,d**). This degenerative process commenced at 6 weeks of age and was completed by 10 weeks of age. There was some variation in the distribution of affected cardiomyocytes, but penetrance of the phenotype was almost 100%. Histologically, degradation of cardiomyocytes and macrophage infiltration were observed at the border between the fibrosis and the viable myocardial tissue (**Fig. 1e,g**), indicating that cardiomyocyte degeneration proceeded from the outer part of the right ventricular wall to the inner part. This outer-inner progression of RVD is also characteristic of human ARVD. Thin fibrous tissue surrounded the degraded cardiomyocytes at the

[1]Department of Internal Medicine and Therapeutics, Osaka University Graduate School of Medicine, 2-2 A8 Yamadaoka, Suita, Osaka 565-0871, Japan. [2]Cardiovascular Division of Internal Medicine, National Cardiovascular Center, 5-7-1 Fujishirodai, Suita, Osaka 565-8565, Japan. [3]Laboratory for Genome Exploration Research Group, RIKEN Genomic Sciences Center (GSC), RIKEN Yokohama Institute, Yokohama, Kanagawa 230-0045, Japan. [4]Department of Gene Therapy Science, Osaka University Graduate School of Medicine, 2-2 Yamadaoka, Suita, Osaka 565-0871, Japan. [5]Department of Nutrition and Physiological Chemistry, Osaka University Graduate School of Medicine, 2-2 Yamadaoka, Suita, Osaka 565-0871, Japan. Correspondence should be addressed to M.K. (kitakaze@zf6.so-net.ne.jp) or S.T. (takasima@medone.med.osaka-u.ac.jp).

Published online 18 January 2004; doi:10.1038/ng1294

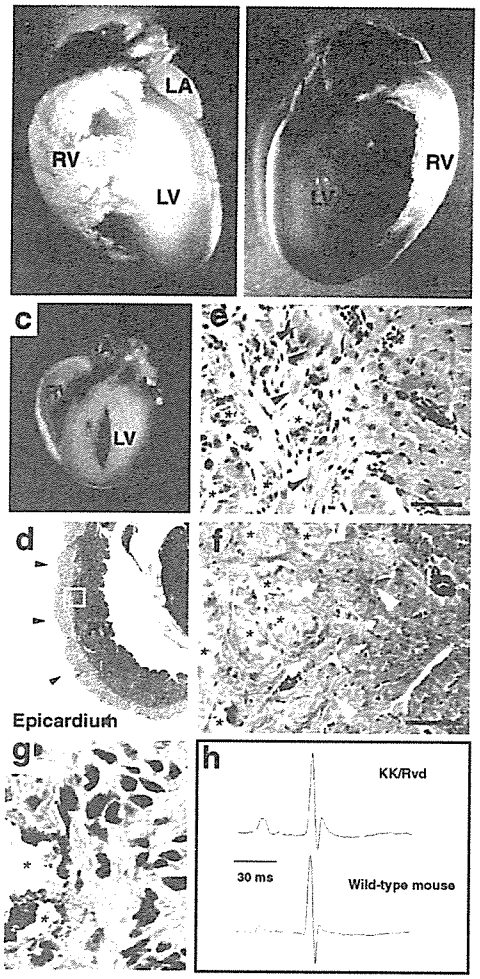

Figure 1 Massive fibrosis covers the outer side of the right ventricular wall, as with human ARVD, and never extends to the left ventricle. Macroscopic view of KK/Rvd mouse heart at 8 weeks old: (**a**) front view, (**b**) back view. (**c**,**d**) In the sagittal section, arrowheads indicate the degenerated area of the right ventricle. (**e**,**f**) At the borderline of the degenerated area (high magnification of yellow square in **d**), green arrows indicate the cardiomyocytes densely stained by eosin; yellow arrows indicate the degraded cardiomyocytes surrounded by fibrous tissue; asterisks indicate calcification. (**e**) Hematoxylin and eosin staining. (**f**) Masson-trichrome staining. (**g**) Infiltrating macrophages into a degraded area are stained by MCP-1 antibody. (**h**) Electrocardiography showed a prolonged QRS duration in KK/Rvd mice. LA, left atrium; LV, left ventricle; RA, right atrium; RV, right ventricle. Scale bars: **a**–**c**, 3 mm; **e**,**f**, 50 μm; **g**, 10 μm.

edge of the myocardial degeneration (**Fig. 1f**), indicating progressive replacement by fibrous tissue.

As lymphocyte infiltration was rarely observed, even when immunohistochemical staining was used (data not shown), autoimmune and infectious mechanisms were probably not involved. Detailed microscopic examination showed that the left ventricular myocardium was intact without any of the changes seen in the right ventricular myocardium. Electrocardiography showed a prolonged QRS duration (duration of ventricular muscle depolarization) in KK/Rvd mice compared with wild-type mice (**Fig. 1h**); this indicated a greater susceptibility to arrhythmia caused by intraventricular conduction disturbance. But electrocardiographic monitoring did not detect tachyarrhythmia, which is often seen in human ARVD. The other organs of these mice showed no histological abnormalities. Thus, KK/Rvd mice matched three of the primary clinical criteria for ARVD[15]: regional right ventricular dysplasia, inheritability and fibro-fatty replacement. Thus we concluded that this was an appropriate mouse model of human ARVD.

Identification of the locus underlying RVD

To investigate the mode of inheritance of RVD, we carried out a cross test between the wild-type PWK mouse strain and the KK/Rvd strain. F_1 mice showed no RVD, whereas the segregation ratio of normal to RVD mice among the F_2 and backcross progeny indicated that RVD was inherited as an autosomal recessive trait. We named the associated locus 'right ventricular dysplasia' (*rvd*). Linkage analysis of these backcross mice (n = 480) with the use of 165 microsatellite markers showed that the *rvd* locus was closely linked to *D7Mit270* near the middle of chromosome 7, with a maximum multipoint odds score of 4.67 (**Fig. 2a**). Using other markers deduced from the gene databases flanked with *D7Mit270*, we further genotyped these mice and localized the recombinants to a region of ~3.0 cM.

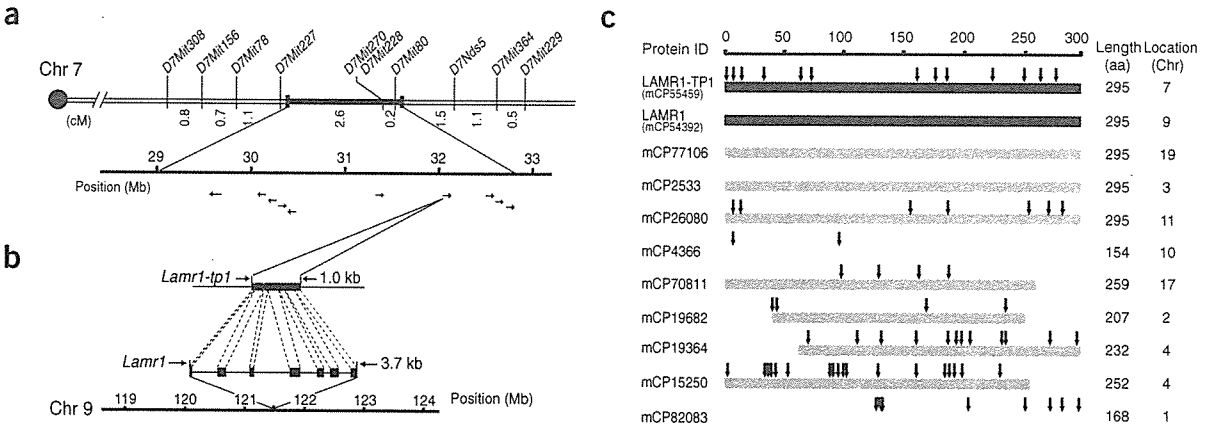

Figure 2 Location, alignment and expression of *Lamr1-tp1*. (**a**) The *rvd* locus was mapped to mouse chromosome 7, linking to *D7Mit270*. (**b**) Sequence of 1,031 bp was inserted in the KK/Rvd mouse genome but not in the PWK mouse genome. (**c**) Alignments of *Lamr1* retroposons in the mouse genome database and the comparison of translated amino acid (aa) sequences to the LAMR1 sequence (from the original *Lamr1* gene located in chromosome 9). Arrows indicate the amino acid transitions.

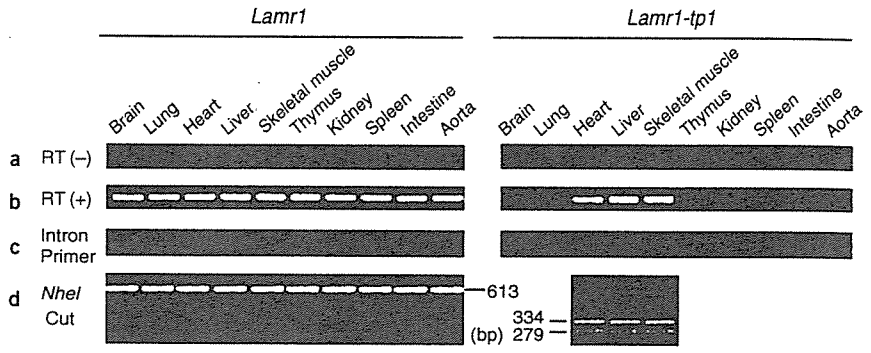

Figure 3 The expression of *Lamr1-tpl* was confirmed only in KK/Rvd heart, liver and skeletal muscle. (**a**) RT(–) indicates the use of RNA samples from KK/Rvd tissues as the PCR template before RT-PCR. PCR primers were designed to include either *Lamr1*- or *Lamr1-tpl*-specific mutated sequences. (**b**) RT(+) indicates the use of the cDNA samples after RT-PCR. The primers were the same as in **a**. (**c**) The same templates were used as in **b**, but reaction primers were designed in the intron lesion of *Lamr1* or up- or downstream of *Lamr1-tpl*. (**d**) PCR products of **b** were digested by the restriction enzyme *Nhe*I, whose recognition site exists only in *Lamr1-tpl*.

Then we sequenced the exons of the *rvd* locus in the gene database and compared the sequences between KK/Rvd and PWK mice. New differences between the two strains shown by this analysis were used as markers to narrow the candidate locus. Within the narrowed region (0.5 cM) we found a 1,031-bp insertion in the KK/Rvd genome that was not present in the PWK genome (**Fig. 2b**). This insert was a 1,031-bp retroposon that encoded mutated *Lamr1*, which we named *Lamr1-tpl* (laminin receptor 1, transposed paralog 1). There was neither an annotated area nor a dbEST matched area within ~1 Mb of this insertion, indicating that alteration of a nearby gene was probably not the cause of this phenotype and suggesting that *Lamr1-tpl* itself was responsible for RVD.

The original *Lamr1* gene consists of seven exons and six introns located on chromosome 9, and it comprises 32 variants of retroposons that are probably derived from a retrovirus. The alignments of these paralogs of *Lamr1* are shown (**Fig. 2c**). Almost all the retroposons have stop codons in the open reading frame and thus are probably not translated. But four *Lamr1* retroposons, including *Lamr1-tpl*, have the stop codon in the same position as the *Lamr1* cDNA. This suggests that these genes could be translated to produce proteins with various mutations. Among the four full-length retroposons, two genes have exactly the same sequence as *Lamr1* and two genes encode mutated *Lamr1* (one of these is *Lamr1-tpl* located on chromosome 7 in KK/Rvd mice and the other is located on chromosome 11). The protein encoded by *Lamr1-tpl* (LAMR1-TP1) shares 96% sequence identity with the protein encoded by *Lamr1* (LAMR1), resulting in the translation of a protein showing a 13–amino acid mutation.

Tissue expression of *Lamr1-tpl*

For *Lamr1-tpl* to cause ARVD, this retroposon would need to be transcribed in the hearts of KK/Rvd mice. We used specific RT-PCR to amplify *Lamr1-tpl* and *Lamr1* transcripts. We isolated RNA and treated it with DNase to eliminate contamination by genomic DNA before RT-PCR. We confirmed the absence of contamination using several PCR reactions with different pairs of intron primers. *Lamr1-tpl* mRNA could only be transcribed in the heart, liver and skeletal muscle of KK/Rvd mice, whereas *Lamr1* mRNA was expressed ubiquitously (**Fig. 3**). Also, *Lamr1-tpl* was not transcribed in any of the tissues of PWK mice or other wild-type (C57Bl/6) mice. There was no difference in the expression of *Lamr1-tpl* in the right ventricle and left ventricle, suggesting that an additional factor was necessary to cause the specific pathological changes associated with ARVD. Despite the high expression of *Lamr1-tpl* transcripts, no pathology was observed in the liver and skeletal muscle of KK/Rvd mice.

In vivo role of LAMR1-TP1

To confirm that the *Lamr1-tpl* transcripts were responsible for the ARVD phenotype, we carried out functional studies of LAMR1-TP1. We transfected a green fluorescent protein (GFP) coexpression plasmid (pIRES2EGFP-Lamr1-tp1 or pIRES2EGFP-Lamr1) into the hearts of C57Bl/6 mice by direct injection of DNA into the right ventricle as described[16]. Three weeks after transfection, we detected expression of LAMR1-TP1 along with massive right ventricular wall damage at the injected area. We observed GFP^+ cardiomyocytes transfected with pIRES2EGFP-Lamr1-tp1 in the zone of degeneration accompanied by fibrosis (**Fig. 4a–c**). The degeneration of transfected cardiomyocytes started 2 weeks after injection of the plasmid. Lymphocyte infiltration was rarely seen in the injected area, and the same changes were also observed in immunosuppressed severe-combined immunodeficient mice (data not shown), suggesting that autoimmunity was probably not involved in this tissue damage. On the other hand, the hearts injected with plasmid pIRES2EGFP-Lamr1

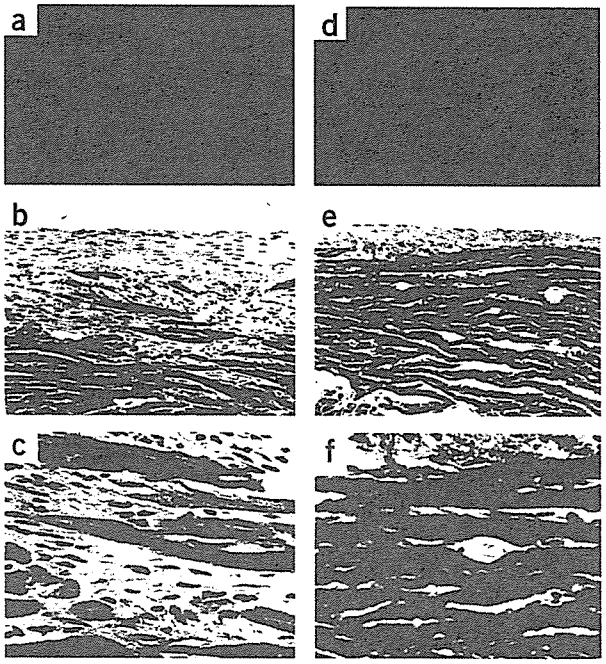

Figure 4 The direct gene injections showed the *Lamr1-tpl*-specific degradation of the myocardium. (**a**,**d**) GFP expression was detected in the gene-injected area. (**b**,**e**) Macroscopic view of transfected sites. (**c**,**f**) Magnified view of the transfected sites. (**a–c**) The vector pIRES2EGFP-Lamr1-tp1 was used. (**d–f**) The vector pIRES2EGFP-Lamr1 was used. Magnification: **a**,**d**, ×40; **b**,**e**, ×100; **c**,**f**, ×400.

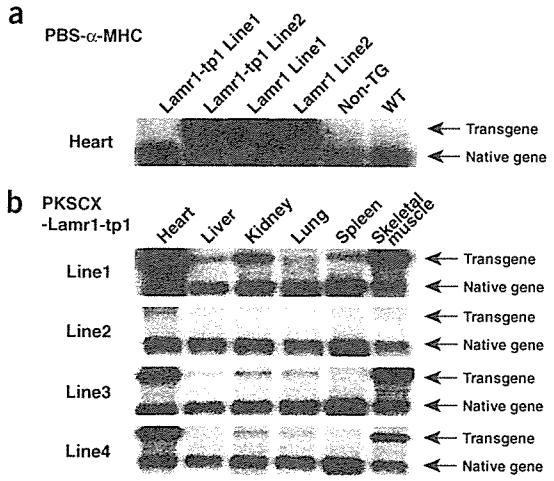

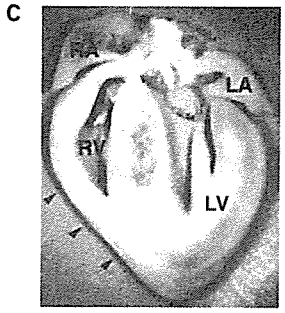

PBS-α-MHC-Lamr1-tp1 heart

Figure 5 Expressional (northern blot) analysis both of the transgenes and native genes in each transgenic mouse model. *Lamr1-tp1* and *Lamr1* were detected in equal amounts in this analysis. (**a**) Transgene expression in heart samples from two strains of PBS-α-MHC-Lamr1-tp1 mice, two strains of PBS-α-MHC-Lamr1 mice and a control (WT) mouse strain. Non-TG, nontransgenic strain. (**b**) Comparison of gene expression by four lines of the transgenic mouse model PKSCX-Lamr1-tp1 in which transgenes were systemically expressed. (**c**) The complete change to the right ventricle is shown in a macroscopic view of a PBS-α-MHC-Lamr1-tp1 heart from a 10-week-old mouse. LA, left atrium; LV, left ventricle; RA, right atrium; RV, right ventricle.

showed only slight damage at the injection site and the GPF$^+$ cells were healthy, showing no degradation (**Fig. 4d–f**). Fibrous tissue was rarely seen in the hearts transfected with *Lamr1*.

We analyzed further the role of LAMR1-TP1 using transgenic mice. We generated two strains of transgenic mice that expressed *Lamr1* either systemically (with a KSCX promoter) or only in the heart (with an α-MHC promoter). We then established six substrains of *Lamr1-tp1* transgenic mice (four with KSCX promoters and two with α-MHC promoters) and four substrains of *Lamr1* transgenic mice (**Fig. 5a,b**). Among the six strains of *Lamr1-tp1* transgenic mice, four strains showed cardiac expression of the LAMR1-TP1 product.

All four strains expressed LAMR1-TP1 in the heart and were extremely susceptible to RVD (**Fig. 5c**). Sometimes the tissue damage extended to the left ventricle, but right ventricle involvement was always predominant. So far, no phenotypic changes have been detected in the other organs of *Lamr1-tp1* transgenic mice. In contrast, all strains that expressed LAMR1 showed no marked changes in any organ, including the heart. These data indicated that LAMR1-TP1 was responsible for RVD in KK/Rvd mice.

In vitro role of LAMR1-TP1

The *in vitro* expression of LAMR1-TP1 also impaired cardiomyocyte function. Cultured rat cardiomyocytes were transfected with an adenovirus vector containing Lamr1-tp1-IRES-GFP and Lamr1-IRES-GFP under the control of a CA promoter. To clarify the effects of these constructs, we carried out an MTS assay. Only expression of *Lamr1-tp1* by cardiomyocytes led to a decrease of cell numbers 48 h after transfection (**Fig. 6a**), even though the same transfection efficiency was confirmed in all groups based on the level of GFP expression (**Fig. 6b**). On histochemical staining, the most prominent change in these cells was alteration of the chromatin architecture. Staining of heterochromatin by DAPI showed a mosaic pattern in cardiomyocytes transfected with *Lamr1* and a speckled pattern in cardiomyocytes transfected with *Lamr1-tp1*.

We analyzed the localization of LAMR1 and LAMR1-TP1 by confocal microscopy. Rat cardiomyocytes transfected with an adenovirus vector were stained using a LAMR1 antibody (FD4818). This antibody could not distinguish LAMR1 from LAMR1-TP1, but only transfected proteins were stained because endogenous LAMR1 was not detected at its relatively low level of expression. LAMR1 was identified in the DAPI-negative euchromatin area of the nucleus, showing a mirror image to the pattern of DAPI staining (**Fig. 6c**). On the other hand, transfection with *Lamr1-tp1* altered the overall pattern of chromatin as described above and LAMR1-TP1 was partially colocalized with the DAPI-positive heterochromatic loci (**Fig. 6c**). These structural changes to chromatin were observed 10–12 h after transfection and preceded the onset of decreasing cell numbers 24 h after transfection.

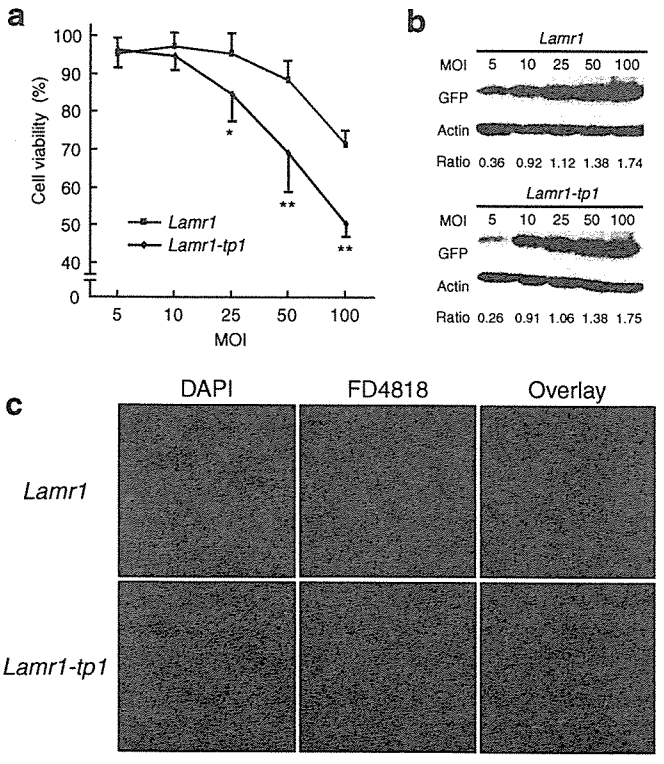

Figure 6 *Lamr1-tp1* caused cardiomyocyte cell death. Cardiomyocytes were infected with recombinant adenoviruses at the indicated multiplicity of infection (MOI). (**a**) Cells expressing *Lamr1-tp1* show lower MTS activity 48 h after adenovirus infection. $^*P < 0.05$ versus *Lamr1*; $^{**}P < 0.005$ versus *Lamr1*. (**b**) GFP and actin expression were analyzed 8 h after adenovirus infection. Cell numbers were equivalent at this time point. The ratios of densitometric measurement of GFP:actin are indicated. (**c**) The nuclei of rat cardiomyocytes expressing Lamr1-IRES-GFP or Lamr1-tp1-IRES-GFP were stained with the LAMR1 antibody FD4818 (green) and DAPI (blue). LAMR1 staining showed a perfect mirror image to DAPI-positive area. LAMR1-TP1 was translocated and partially overlapped with DAPI-positive. Scale bar, 20 μm.

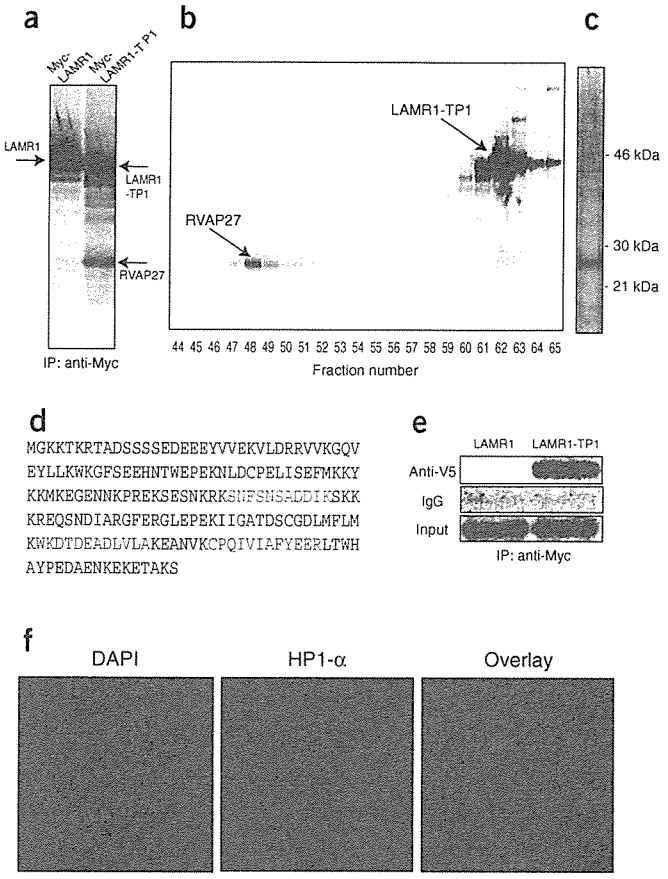

Figure 7 LAMR1-TP1 interacts with HP1-α. (**a**) RVAP27 was immunoprecipitated with LAMR1-TP1 but not with LAMR1 in COS7 cells labeled by ^{35}S-cystein and methionine. (**b**) The complex of radiolabeled LAMR1-TP1 and RVAP27 was separated by a phenyl reverse-phase column. (**c**) The final purification product of RVAP27 was silver-stained. (**d**) The peptides derived from the purified protein, which fitted with those of human HP1-α (as assessed by direct N-terminal sequencing (red) or liquid chromatography-mass spectrometry or mass spectrometry (blue)), are underlined. Cytokine was detected as a Cys-S-propionamide. (**e**) V_5-LAMR1-TP1 but not V_5-LAMR1 expressed in COS7 cells was immunoprecipitated with Myc-tagged HP1-α by anti-Myc. IgG was derived from nonimmunized serum. (**f**) Rat cardiomyocytes were stained with HP1-α antibody, showing HP1-α localization with the DAPI-positive heterochromatin area.

The data suggested that these chromatin changes might have had a lethal effect on the cardiomyocytes, although the possibility that these changes were secondary to lethal cell damage itself cannot be fully excluded.

HP1 binds to mutant LAMR1

To clarify the cellular mechanism by which LAMR1-TP1 caused conformational changes of heterochromatin, we purified and cloned the protein specifically interacting with LAMR1-TP1. The Myc-tagged LAMR1-TP1 fusion protein expressed in ^{35}S-labeled COS7 cells showed the same migration pattern as Myc-tagged LAMR1 (**Fig. 7a**). This 27-kDa protein (named RVAP27) was immunoprecipitated with LAMR1-TP1 but not with LAMR1. Using either a mouse cell line (3T3) or rat cardiomyocytes, we also immunoprecipitated RVAP27 with transfected LAMR1-TP1. Large-scale purification of RVAP27 was done by the sequential use of columns (**Fig. 7b**), and about 10 pmol of RVAP27 was purified from the lysate of 1.0×10^8 COS7 cells (**Fig. 7c**). We analyzed the peptides digested from the RVAP27 band by Edman degradation N-terminal sequencing or nanoelectrospray ionization tandem mass spectrometry. RVAP27 included fragments of the amino acid sequences of SNFSNSADDIK, WKDTDEADLVLA and CPQIVIAFYEER that matched human heterochromatin protein 1-α (HP1-α) (**Fig. 7d**). The Myc antibody coprecipitated Myc-tagged HP1-α with V_5-tagged LAMR1-TP1, but not with LAMR1; this verified the specific interaction between HP1-α and LAMR1-TP1 (**Fig. 7e**).

HP1 is a key heterochromatin protein that regulates gene silencing by interacting with methylated histones[17]. HP1-α also localizes with DAPI-positive heterochromatin[18]. Cardiomyocytes expressing HP1-α showed the same staining pattern in the DAPI-dense region (**Fig. 7f**). Our immunohistochemical data showed that LAMR1 localized to the euchromatin (DAPI-negative) and that LAMR1-TP1 was partially translocated to heterochromatin (DAPI-positive; **Fig. 6c**). These findings imply that the mutant LAMR1 had an increased affinity for HP1-α and thus was translocated to heterochromatin. Such translocation might influence transcriptional regulation and interfere with the expression of genes essential to the survival of cardiomyocytes, leading to lethal cell dysfunction due to LAMR1-TP1.

Changes of gene expression induced by LAMR1-TP1

To investigate transcriptional regulation by LAMR1-TP1, we analyzed changes in gene expression in cultured cardiomyocytes after transfection of *Lamr1-tp1* or *Lamr1*. Because cells expressing *Lamr1-tp1* began to die 24 h after transfection, we analyzed gene expression at 6 h, 12 h and 24 h (each in duplicate) to exclude the secondary effects of lethal cell damage. GFP expression indicated that the transfected protein was expressed 10 h after transfection, indicating that the expression of genes at 6 h was largely induced by viral infection itself. Transfection with wild-type LAMR1 had a minimal effect on the expression profile compared with that of nontransfected cardiomyocytes, even though the adenovirus vector itself should cause some cell damage (**Supplementary Fig. 1** online). On the other hand, LAMR1-TP1 caused substantial changes in gene expression at 12 h and 24 h, but not at 6 h (**Supplementary Table 1** online). These genes showed similar changes in expression in duplicate analyses. We confirmed further the expression of these genes by quantitative PCR (**Supplementary Fig. 1** online). Our results suggested that LAMR1-TP1, but not LAMR1, could alter the expression of some specific genes. How these genes actually determine the fate of cardiomyocytes needs to be determined in order to understand the pathological role of this mutant protein.

DISCUSSION

Although lethal tachyarrhythmia is often detected in human ARVD, we did not detect it in this mouse model. The difficulty in generating lethal tachyarrhythmia in mice, due to the high beating rate and small size of their hearts[19], might explain our failure to detect lethal arrhythmia. KK/Rvd mice showed electric conduction inhomogeneity leading to prolonged QRS duration, which is often seen in humans with ARVD[20,21]. If similar degradation occurs in the human heart, it will become a focus for lethal arrhythmia at some stage in life. The most important pathological feature of ARVD is the degeneration of right ventricular cardiomyocytes[22]. Our ARVD mouse model reproduced the specific right ventricular degeneration from the outside inwards.

It is still not known why the right ventricle is more susceptible than the left ventricle in these mice. Injection of *Lamr1-tp1* into the left ventricle also induced cardiomyocyte degeneration and calcification,

Table 1 Comparison of human *LAMR1* and histone-related gene loci with ARVD loci

ARVD candidate locus	*LAMR1* related gene	Histone-related gene
ARVD4, 2q32.1–32.3	XM_013127*, 2q31	*HAT1*, 2q31.2–33.1
ARVD5, 3p23	*LAMR1*, 3p21	
ARVD6, 10p12–14	XM_053952*, 10p14	

HAT1, histone acetyl transferase 1; asterisks, *LAMR1* retroposons.

but the changes were less severe (data not shown). Also, transgenic mice that expressed LAMR1-TP1 in both cardiac chambers showed predominant right ventricular degeneration. It seems possible that the threshold for cardiomyocyte damage is higher in the left ventricle than in the right ventricle. This implies that a higher level of *Lamr1-tp1* expression could cause left ventricular degeneration. Often in human ARVD, a part of the left ventricle is involved. Although both ARVD2 and Naxos disease show a right ventricle–specific phenotype in humans, the genes responsible are equally expressed in both cardiac chambers[6,23]; the mechanism of right ventricular susceptibility is still unknown. The most likely explanation is that specific genes that determine the susceptibility to cell damage exist in either ventricle. Left ventricular cardiomyocytes are under high stress because of the high pressure in this ventricle, and more cytoprotective genes may be induced as a result. In fact, microarray analysis comparing right ventricle and left ventricle shows higher expression in the left ventricle of genes belonging to the category of cell and organism defense[24]. Dominant degeneration of the outer right ventricular wall in ARVD also supports this concept because the inner free wall is under more mechanical stress and expresses more defensive genes, such as heat shock proteins. This mechanism might lead to left ventricle protection in ARVD. Alternatively, right ventricle–specific genes may be involved in the susceptibility of the right ventricle. Mice lacking the right ventricle–specific gene actinin-associated LIM-domain protein show some ARVD-like features[25], even though the histological characteristics are considerably different from those of human ARVD.

We found that one of the heterochromatin complex proteins, HP1-α, showed specific binding to LAMR1-TP1. HP1-α is a key component of condensed DNA and is involved in gene silencing by interaction with methylated histone H3. Mobility of HP1-α has been reported in various cells[18,26]. The stochastic competition between such factors as LAMR1-TP1 and HP1-α may determine the fate of the heterochromatin plasticity that is involved in regulating the fate of cells. Class II histone deacetylase acts as a signal-responsive suppressor of the transcriptional events governing cardiac hypertrophy and heart failure[27]. HP1 can link with class II histone deacetylase[28] and thus may modify cardiac cell metabolism. Accordingly, we conclude that LAMR1-TP1 was translated from an active retroposon in ARVD mice and then interacted with HP1-α, leading to the early death of cardiomyocytes.

Genomic databases indicate that there are up to 40 and 32 *Lamr1* retroposons in humans and mice, respectively. It has also been suggested that the *Lamr1* gene family in mammals, with the exception of the functional locus, is comprised entirely of retrotransposons or processed pseudogenes. Most processed retroposons are not expressed and have no functional activity, but several active retroposons or pseudogenes have been identified[29–32]. We show that the active retroposon may cause the pathological condition of ARVD. In humans, a highly conserved mutated form of *Lamr1* has been isolated from a fetal brain cDNA library[33], suggesting that mutant LAMR1 proteins are also transcribed in humans. Several reported human ARVD loci are located close to the retroposons of *Lamr1* or histone-modulating protein genes (**Table 1**), suggesting that either LAMR1 or HP1 may cause hereditary RVD in humans.

METHODS

PWK mouse strain. The PWK strain belongs to the *Mus musculus musculus* subspecies, which separated from *Mus musculus domesticus* some 1 million years ago. It is maintained as one of the wild-type–derived inbred strains.

***Lamr1-tp1* expressional analysis.** We carried out PCR assays to confirm the presence of each identified mutation. Mismatch assays for the 287T→C and 291G→T mutations in the nucleic acid sequence of *Lamr1* introduced changes at the penultimate 3′ position for the forward primer and 868C→T for the reverse primer, respectively (primer sequences available on request). Each PCR product was digested with *Nhe*I (specific for *Lamr1-tp1* amplicon) to produce fragments of 334 bp and 279 bp; the *Lamr1* amplicon was uncut.

Injection of recombinant DNA *in vivo*. Female C57Bl/6 mice (8 weeks old, 22–25 g) were anesthetized with a mixture of ketamine (100 mg per kg body weight intraperitoneally) and xylazine (5 mg kg body weight intraperitoneally), intubated and ventilated. We carried out a left lateral thoracotomy to expose the beating heart and injected 10 μg of plasmid DNA in 100 μl of phosphate-buffered saline containing 5% sucrose into the right ventricular wall with a 30-gauge needle. The mice were killed 3 weeks after injection and histological staining was done.

Transgenic mice models. We constructed three kinds of targeting vectors under the following promoters (*Lamr1-tp1*, KSCX and α-MHC; *Lamr1*, α-MHC). We introduced these targeting vectors into blastocysts (derived from the C57Bl/6 Jcl mouse strain) by a standard pronuclear microinjection technique[34].

Preparation of adenovirus. Replication-defective recombinant adenoviral vectors expressing Lamr1-tp1-IRES-GFP and Lamr1-IRES-GFP were prepared with the adenovirus expression vector kit following the manufacturer's protocol (Takara). Briefly, *Lamr1-tp1* and *Lamr1* cDNA connected to an IRES-GFP sequence (Clontech) were placed after a CA promoter that was composed of a cytomegalovirus enhancer; a chicken β-actin promoter and rabbit β-globin poly(A) were inserted into a cassette cosmid vector that contained an entire adenovirus type 5 genome except for the E1a, E1b and E3 regions. A recombinant adenovirus was constructed by *in vitro* homologous recombination in HEK293 cells with the use of this cosmid vector and the adenovirus DNA terminal-protein complex. The desired recombinant adenovirus was purified by ultracentrifugation through a $CsCl_2$ gradient followed by extensive dialysis. The titer of the virus stock was assessed by a plaque formation assay that used the HEK293 cells. Cardiomyocytes were infected with the recombinant adenovirus vectors at a multiplicity of infection of 5–100 plaque-forming units per cell. We assessed the expression of GFP and β-actin by immunoblotting with 20 μg of myocardial protein lysate.

Primary culture of neonatal rat ventricular myocytes and MTS assay. Ventricular myocytes obtained from 1- or 2-d-old Wister rats were prepared and cultured overnight in Dulbecco's modified Eagle medium containing 10% fetal bovine serum as described[35]. Cytotoxicity was assessed with a CellTiter 96 Aqueous One Solution Cell Proliferation Assay System (Promega). Rat cardiomyocytes were cultured in 96-well culture plates at a density of 3×10^4 cells cm^{-2}. MTS reagent was added to each well 48 h after the addition of adenovirus to the myocytes. After a 1-h incubation period, optical absorbance at 490 nm was measured with a microplate reader. Cell viability was expressed as mean percentages for the absorbance at multiplicity of infection of 5 with the standard deviations of absorbance.

Antibodies. We used antibodies to MCP-1 (Santa Cruz Biotechnology), GFP, Myc-conjugate beads (Clontech), V_5 (Invitrogen) and HP1-α (Upstate Biotechnology). The polyclonal antibody FD4818 was derived from rabbits against the amino acid sequence RALNVLQMKEEDVFK, which corresponds to amino acids 3–15 of LAMR1.

Identification of LAMR1-TP1 binding protein (RVAP27). We metabolically labeled 2.0×10^5 COS7 cells expressing either PCDNA3.1-Myc-tagged-Lamr1 or PCDNA3.1-Myc-tagged-Lamr1-tp1 (Invitrogen) with ^{35}S, lysed them with 1 ml of lysis buffer (20 mM Tris pH 8.0, 5% acetonitrile, 5 M MEDTA, 1% Nonidet P-40) and immunoprecipitated them with a Myc antibody. Bound materials were separated by SDS-PAGE and the radioactivity was detected by a BAS imaging analyzer (Fuji). The eluted fraction from Myc-antibody beads was also injected onto a Phenyl-RPLC column (4.6 × 250mm, Nakarai) equilibrated with 0.1% trifluoroacetic acid and 5% acetonitrile. Fractions were eluted with a linear gradient of 27–37% acetonitrile at a flow rate of 1 ml. Each fraction was lyophilized and separated by SDS-PAGE. Radioactivity was detected by BAS imaging system.

Large-scale purification and sequence analysis of LAMR1-TP1–binding protein. COS7 cells (1.0×10^8) expressing Myc-tagged LAMR1-TP1 were lysed with 200 ml of lysis buffer and applied to 500 µl of Myc-antibody beads (Clontech). Bound materials were eluted with 0.1% trifluoroacetic acid and 5% acetonitrile. The eluted fraction was diluted 50 times with a lysis buffer and was applied to Uno-Q anion exchange column (Bio-Rad). The column was equilibrated with 20 mM Tris and 5% acetonitrile at pH 8.0 and bound materials were eluted with a linear gradient of NaCl (0–0.5 M) at a flow rate of 1 ml min^{-1}. Five fractions of about 0.3 M NaCl elution were pooled and injected onto a Phenyl-RPLC column (4.6 × 250 mm, Nakarai) equilibrated with 0.1% trifluoroacetic acid and 5% acetonitrile. Fractions were eluted with a linear gradient of 27–37% acetonitrile at a flow rate of 1 ml. After separating by SDS-PAGE, RVAP27 was eluted at the same fraction in which the radioactive LAMR1-TP1 was detected. Purified RVAP (10 pmol) was subjected to SDS-PAGE on 12% gel. After staining the gel with SyproRuby, the 27-kDa band was cut and treated with trypsin. The tryptic digest was fractionated by nanoscale HPLC on a C18 column (0.1 × 50 mm). Two fractions were analyzed by direct N-terminal sequence by Edman degradation with the HP G1005 Protein Sequencing System. One fraction was analyzed with a tandem mass spectrometer (Q-Tof2) equipped with a nanoelectrospray ionization source. Positive ion tandem mass spectra were measured.

RNA preparation and hybridization to oligonucleotide arrays. Total RNA was isolated from viable mice or cultured neonatal cardiomyocytes derived from C57Bl/6 mice. Affymetrix Gene Chip technology was used as described[36]. Briefly, cDNA was synthesized from total RNA and annealed to a T7-oligo-dT primer. Reverse transcription was done with Superscript II reverse transcriptase. Second-strand cDNA synthesis was done with DNA polymerase I with the appropriate reagents. Synthesis of biotin-labeled cRNA was done by *in vitro* transcription with the MEGAscript T7 IVT Kit (Ambion, Inc). The cRNA was fragmented and hybridized to GeneChip Murine U74vA2 Array Set (Affymetrix). Hybridization, probe washing, staining and probe array scan were done according to the protocols provided by Affymetrix. Detailed information about the array protocol and data is available in the GEO database (see URL and accession number below).

Real-time PCR. Real-time PCR was done with TaqMan technology and the ABI Prism 7700 Detection System (Applied Biosystems). Reactions (25 µl) were set up using the 2× Universal PCR Master Mix (Applied Biosystems), template cDNA and adequate concentrations of primers and probes. All of the samples were processed in duplicate. To standardize the quantity of the two selected genes, GAPDH was used as the endogenous control reference because our microarray analysis showed that the level of GAPDH was stable and no significant difference was noted among all the three groups.

Data analysis. GeneSpring 5.0 (Silicon Genetics) software was used for analyses. A global normalization was used for all data in the 18 arrays with a combination of three steps: transforming negative values to 0.01, normalizing to the 50th percentile per chip and normalizing to median per gene. We filtered data using a combination of signal confidence ('present' flag), relative change (1.5–2.0 times), minimum acceptable signal intensity (average difference ≥50 in at least one of three groups) and a statistical cut-off ($P < 0.05$, Student's *t*-test). Data are presented as mean or mean ± s.e.m.; the one-way ANOVA with Tukey-Kramer exact probability test was used to test the differences among all the groups and the least-squares method was used to determine linear correlation between selected variables. $P < 0.05$ was considered statistically significant.

Animal experiments. All animal experiments were approved by the Institutional Animal Care and Use Committee at Osaka University Graduate School of Medicine.

URL. The GEO database is available at http://www.ncbi.nlm.nih.gov/geo/.

GEO accession number. GSE927.

Note: Supplementary information is available on the Nature Genetics website.

ACKNOWLEDGMENTS

These data were generated through the use of the Celera Discovery System and Celera Genomics' Associated Databases. We thank T. Tanaka and K. Miyake for assistance with DNA sequencing; S. Hirota for histologic expertise; H. Niwa for donating plasmid constructs and providing suggestions; K. Yamamoto for amino-acid sequencing; and H. Kikutani, K. Node and T. Nakagawa for discussions. This work was supported by Grants-in-aid for Scientific Research from the Japanese Ministry of Education, Culture, Sports, Science and Technology and from the Ministry of Health and Labor and Welfare, Japan.

COMPETING INTERESTS STATEMENT

The authors declare that they have no competing financial interests.

Received 20 November; accepted 29 December 2003
Published online at http://www.nature.com/naturegenetics/

1. Thiene, G. *et al.* Arrythmogenic right ventricular cardiomyopathy. *Trends Cardiovasc. Med.* **7**, 84–90 (1997).
2. Severini, G.M. *et al.* A new locus for arrhythmogenic right ventricular dysplasia on the long arm of chromosome 14. *Genomics* **31**, 193–200 (1996).
3. Rampazzo, A. *et al.* ARVD4, a new locus for arrhythmogenic right ventricular cardiomyopathy, maps to chromosome 2 long arm. *Genomics* **45**, 259–263 (1997).
4. Ahmad, F. *et al.* Localization of a gene responsible for arrhythmogenic right ventricular dysplasia to chromosome 3p23. *Circulation* **98**, 2791–2795 (1998).
5. Li, D. *et al.* The locus of a novel gene responsible for arrhythmogenic right- ventricular dysplasia characterized by early onset and high penetrance maps to chromosome 10p12-p14. *Am. J. Hum. Genet.* **66**, 148–156 (2000).
6. Tiso, N. *et al.* Identification of mutations in the cardiac ryanodine receptor gene in families affected with arrhythmogenic right ventricular cardiomyopathy type 2 (ARVD2). *Hum. Mol. Genet.* **10**, 189–194 (2001).
7. Bright, J.M. & McEntee, M. Isolated right ventricular cardiomyopathy in a dog. *J. Am. Vet. Med. Assoc.* **207**, 64–66 (1995).
8. Simpson, K.W., Bonagura, J.D. & Eaton, K.A. Right ventricular cardiomyopathy in a dog. *J. Vet. Intern. Med.* **8**, 306–309 (1994).
9. Fox, P.R., Maron, B.J., Basso, C., Liu, S.K. & Thiene, G. Spontaneously occurring arrhythmogenic right ventricular cardiomyopathy in the domestic cat: A new animal model similar to the human disease. *Circulation* **102**, 1863–1870 (2000).
10. Ishikawa, S., Zu Rhein, G.M. & Gilbert, E.F. Uhl's anomaly in the mink. Partial absence of the right atrial and ventricular myocardium. *Arch. Pathol. Lab. Med.* **101**, 388–390 (1977).
11. Sato, M. *et al.* Analysis of nuclear localization of laminin binding protein precursor p40 (LBP/p40). *Biochem. Biophys. Res. Commun.* **229**, 896–901 (1996).
12. Kaneda, Y. *et al.* The induction of apoptosis in HeLa cells by the loss of LBP-p40. *Cell Death Differ.* **5**, 20–28 (1998).
13. Kondo, K., Nozawa, K., Tomita, T. & Ezaki, K. Inbred strains resulting from Japanese mice. *Bull. Exp. Anim.* **6**, 107–112 (1967).
14. Nakamura, M. & Yamada, K. Studies on a diabetic (KK) strain of the mouse. *Diabetologia* **3**, 212–221 (1967).
15. McKenna, W.J. *et al.* Diagnosis of arrhythmogenic right ventricular dysplasia/cardiomyopathy. Task Force of the Working Group Myocardial and Pericardial Disease of the European Society of Cardiology and of the Scientific Council on Cardiomyopathies of the International Society and Federation of Cardiology. *Br. Heart J.* **71**, 215–218 (1994).
16. Lin, H., Parmacek, M.S., Morle, G., Bolling, S. & Leiden, J.M. Expression of recombinant genes in myocardium in vivo after direct injection of DNA. *Circulation* **82**, 2217–2221 (1990).
17. Nakayama, J., Rice, J.C., Strahl, B.D., Allis, C.D. & Grewal, S.I. Role of histone H3 lysine 9 methylation in epigenetic control of heterochromatin assembly. *Science* **292**, 110–113 (2001).
18. Festenstein, R. *et al.* Modulation of heterochromatin protein 1 dynamics in primary Mammalian cells. *Science* **299**, 719–721 (2003).
19. Cranefield, P. *The Conduction of the Cardiac Impulse* (Futura, Mount Kisco, New York, 1975).
20. Peters, S. & Trummel, M. Diagnosis of arrhythmogenic right ventricular dysplasia-cardiomyopathy: value of standard ECG revisited. *Ann. Noninvasive Electrocardiol.* **8**, 238–245 (2003).

21. Nasir, K. *et al.* Filtered QRS duration on signal-averaged electrocardiography predicts inducibility of ventricular tachycardia in arrhythmogenic right ventricle dysplasia. *Pacing Clin. Electrophysiol.* **26**, 1955–1960 (2003).
22. Burke, A.P., Farb, A., Tashko, G.& Virmani, R. Arrhythmogenic right ventricular cardiomyopathy and fatty replacement of the right ventricular myocardium: are they different diseases? *Circulation* **97**, 1571–1580 (1998).
23. Protonotarios, N. *et al.* Genotype-phenotype assessment in autosomal recessive arrhythmogenic right ventricular cardiomyopathy (Naxos disease) caused by a deletion in plakoglobin. *J. Am. Coll. Cardiol.* **38**, 1477–1484 (2001).
24. Steenman, M. *et al.* Transcriptomal analysis of failing and nonfailing human hearts. *Physiol. Genomics* **12**, 97–112 (2003).
25. Pashmforoush, M. *et al.* Adult mice deficient in actinin-associated LIM-domain protein reveal a developmental pathway for right ventricular cardiomyopathy. *Nat. Med.* **7**, 591–597 (2001).
26. Cheutin, T. *et al.* Maintenance of stable heterochromatin domains by dynamic HP1 binding. *Science* **299**, 721–725 (2003).
27. Zhang, C.L. *et al.* Class II histone deacetylases act as signal-responsive repressors of cardiac hypertrophy. *Cell* **110**, 479–488 (2002).
28. Zhang, C.L., McKinsey, T.A. & Olson, E.N. Association of class II histone deacetylases with heterochromatin protein 1: potential role for histone methylation in control of muscle differentiation. *Mol. Cell. Biol.* **22**, 7302–7312 (2002).
29. McCarrey, J.R. & Thomas, K. Human testis-specific PGK gene lacks introns and possesses characteristics of a processed gene. *Nature* **326**, 501–505 (1987).
30. Gebara, M.M. & McCarrey, J.R. Protein-DNA interactions associated with the onset of testis-specific expression of the mammalian Pgk-2 gene. *Mol. Cell. Biol.* **12**, 1422–1431 (1992).
31. Dahl, H.H., Brown, R.M., Hutchison, W.M., Maragos, C. & Brown, G.K. A testis-specific form of the human pyruvate dehydrogenase E1 α subunit is coded for by an intronless gene on chromosome 4. *Genomics* **8**, 225–232 (1990).
32. Hirotsune, S. *et al.* An expressed pseudogene regulates the messenger-RNA stability of its homologous coding gene. *Nature* **423**, 91–96 (2003).
33. Richardson, M.P., Braybrook, C., Tham, M., Moore, G.E. & Stanier, P. Molecular cloning and characterization of a highly conserved human 67- kDa laminin receptor pseudogene mapping to Xq21.3. *Gene* **206**, 145–150 (1998).
34. Gordon, J.W., Scangos, G.A., Plotkin, D.J., Barbosa, J.A. & Ruddle, F.H. Genetic transformation of mouse embryos by microinjection of purified DNA. *Proc. Natl. Acad. Sci. USA* **77**, 7380–7384 (1980).
35. Simpson, P., McGrath, A. & Savion, S. Myocyte hypertrophy in neonatal rat heart cultures and its regulation by serum and by catecholamines. *Circ. Res.* **51**, 787–801 (1982).
36. Lockhart, D.J. *et al.* Expression monitoring by hybridization to high-density oligonucleotide arrays. *Nat. Biotechnol.* **14**, 1675–1680 (1996).

ELSEVIER

International Journal of Cardiology 97 (2004) 263–276

International Journal of Cardiology

www.elsevier.com/locate/ijcard

Ischemic preconditioning: emerging evidence, controversy, and translational trials

Shoji Sanada[a], Masafumi Kitakaze[a,b,*]

[a] *Department of Internal Medicine and Therapeutics, Osaka University Graduate School of Medicine, Suita, Japan*
[b] *Cardiovascular Division of Medicine, National Cardiovascular Center, Suita, Osaka 565-8565, Japan*

Received 2 October 2003; received in revised form 1 December 2003; accepted 8 December 2003

Abstract

Protection against ischemia by ischemic preconditioning (IP) is seen in many tissues and organs. However, the preconditioning ischemia must precede lethal ischemia for this effect to occur, and the creation of ischemia to treat heart disease does not seem to be a realistic strategy. Accordingly, the underlying mechanisms that confer cardioprotection should be identified. Early studies revealed that IP causes two windows of cardioprotection, and subsequent efforts to detect cardioprotective factors have identified various triggers, mediators, and potent effectors of IP, such as endogenous receptor agonists (adenosine, catecholamines, bradykinin, and opioids), intracellular messengers [protein kinase C (PKC), p38MAPK, PI-3K, and PKA], ion channels such as KATP channels, enzymes including heat shock proteins (HSPs), superoxide dismutase (SOD), and 5′-nucleotidase, and other factors [nitric oxide (NO), growth factors, free radicals, and products of the arachidonic acid cascade]. Some of these factors are involved in several different pathways and may have multiple roles in IP-induced cardioprotection. Recently, however, certain problems have arisen such as controversies related to increasing knowledge and the relative lack of clinical studies in contrast to the intensive performance of basic studies. To overcome these problems, the latest studies have followed three major trends: (1) investigation of mechanisms to explain the current controversies, (2) detection of other unknown potent mechanisms, and (3) promotion of clinical trials based on the evidence from experimental studies in larger animals. Here, we summarize recent investigations on IP, emphasizing on the controversial issues and emerging factors, and discuss current research on the prevention or treatment of ischemic heart disease including some relevant clinical studies.

Keywords: Preconditioning; Adenosine; PKA; PKC; p38MAPK; KATP channel; Clinical trial

1. Introduction

It is very important to determine the mechanism(s) of cardioprotection in diseased hearts because the mortality and morbidity of heart disease are rising around the world, and there is an increasing need for safe, effective, and efficient preventive or therapeutic strategies. In the clinical setting, the treatment of patients with acute coronary syndrome (angina pectoris or acute myocardial infarction) has made dramatic progress following the development and application of percutaneous transluminal coronary angioplasty (PTCA) [1] and percutaneous transluminal coronary recanalization (PTCR) [2]. As a result, mortality related to acute myocardial infarction has decreased, but the functional recovery of reperfused hearts is unfortunately less complete than expected, resulting in an increase of patients with chronic ischemic heart failure [3]. We do not have sufficiently potent drugs or tools to decrease the infarct size and prevent cardiac remodeling in patients with acute myocardial infarction or ischemic heart disease apart from the above recanalization therapies.

Cardiologists involved in the management of patients with acute coronary syndrome, including severe unstable

Abbreviations: Ach, Acetylcholine; R, Receptors; LPS, Lipopolysaccharide; GPCR, G-protein coupled receptors; IGF-1, Insulinlike growth factor-1; 5′-N, Ecto-5′-nucleotidase; ERK, Extracellular signal-regulated kinase; MTP, Mitochondrial transition pore; CREB, cAMP-responsive element binding protein; NHE, Na^+/H^+ exchanger; NCX, Na^+/Ca^{2+} exchanger; VEGF, Vascular endothelial growth factor; COX-2, Cyclooxygenase-2; 12-LO, 12-lipoxygenase; PGs, Prostaglandins; NOS, Nitric oxide synthase; SOD, Super oxide dismutase; HSP, Heat shock protein; GLUT, Glucose transporter.

* Corresponding author. Cardiovascular Division of Medicine, National Cardiovascular Center, 5-7-1 Fujishirodai, Suita, Osaka, 565-8565 Japan. Tel.: +81-6-6833-5012x2225; fax: +81-6-6836-1120.
E-mail address: kitakaze@zf6.so-net.ne.jp (M. Kitakaze).

0167-5273/$ - see front matter © 2003 Elsevier Ireland Ltd. All rights reserved.
doi:10.1016/j.ijcard.2003.12.002

angina and acute myocardial infarction, occasionally used to report "the cardiac warm-up phenomenon" [4], meaning that patients with at least one episode of prodromal angina showed less severe ischemic damage after subsequent exposure to a longer period of ischemia. In 1986, Murry et al. [5] first documented this phenomenon experimentally and termed it "ischemic preconditioning" (IP). Subsequently, numerous studies were performed using various tissues and animals (e.g., liver [6], kidney [7], brain [8], and endothelial cells [9]), and all of them showed that short period(s) of ischemia or anoxia could allow tissues to survive subsequent ischemia that would have otherwise been lethal. The existence of ischemic preconditioning, a ubiquitous finding which is rare in any experimental or clinical field, has made its understanding one of the major targets for prevention of ischemic damage, including acute reversible or irreversible injury, and chronic cardiac dysfunction such as hibernating myocardium or cardiac remodeling [10].

Brief periods of ischemia that cause preconditioning must occur prior to sustained ischemia to achieve cardioprotective effect, but induction of myocardial ischemia is not a realistic treatment for patients with ischemic heart disease. Therefore, the mechanisms underlying ischemic preconditioning need to be determined, so that new strategies can be devised to overcome ischemic insults. If the triggers, mediators, and effectors of ischemic preconditioning could be clarified, it might be easier to develop more effective therapeutic interventions for acute coronary syndrome. Research in this field has been targeting the histological, biochemical, and physiological changes of the myocardium induced by ischemia which provide hints about the cellular mechanisms of ischemic preconditioning. The great efforts of various pioneering investigators and numerous subsequent researchers have already led to considerable progress in understanding the fundamental nature of ischemic preconditioning and possible methods for achieving the goal of cardioprotection.

This article summarizes the history and current status of investigations related to ischemic preconditioning, and then discusses the current topics and controversies as well as the latest clinical research into the treatment of ischemic heart disease.

2. Early studies on ischemic preconditioning

Some of the cardiologists managing patients with acute coronary syndrome, including severe unstable angina and acute myocardial infarction, occasionally observed the so-called "cardiac warm-up phenomenon" [4], which means that patients with at least one episode of prodromal angina subsequently developed less severe chest pain, less prominent S–T segment changes, less severe cardiac dysfunction, or even a smaller infarct size than other patients with a similar duration of myocardial ischemia.

In 1986, Murry et al. [5] studied this phenomenon in a dog model. They reported that brief periods of ischemia accompanied by reperfusion occurring just prior to a sustained ischemic episode could paradoxically lead to the protection of tissues against longer ischemia and to the following changes: (1) delayed depletion of ATP, (2) reduced oxygen consumption, (3) preservation of intracellular structures, and (4) delayed or reduced cellular necrosis caused by a lack of ATP. They termed this phenomenon "preconditioning with ischemia", and their description is now used as the classical definition of ischemic preconditioning. They also found that the extent of protection by ischemic preconditioning was critically dependent on the period between the end of preconditioning ischemia and the onset of sustained ischemia. Thereafter, many studies were performed on various tissues and species [6–9], and all of them confirmed that potent protection against lethal damage due to sustained ischemia was conferred by short period(s) of ischemia or anoxia. Furthermore, an increasing number of studies have shown that the cardioprotection conferred by preconditioning is relevant not only to acute reversible or irreversible injury, such as myocardial stunning or infarction (with necrosis and apoptosis), but also to chronic cardiac disorders such as hibernating myocardium, contractile dysfunction, or remodeling. At present, the definition of ischemic preconditioning has been expanded to include any kind of protection afforded by brief periods of ischemia against damage caused by a subsequent sustained ischemic insult. Ischemic preconditioning has also been demonstrated to occur in humans by some clinical studies [10].

3. Dual preconditioning windows

While initial studies demonstrated that ischemic preconditioning could protect against sustained ischemia that occurred soon after preconditioning, Kuzuya et al. [11] and Marber et al. [12] independently reported in 1993 that the cardioprotective effect of ischemic preconditioning on infarct size was still detectable for 24 h after preconditioning and was associated with the increased expression of high molecular weight cardioprotective heat shock proteins (HSPs) [12]. Because Kuzuya et al. [11] also found that the infarct-limiting effect of preconditioning was lost between 3 and 12 h after a brief period of ischemia, they named these two periods of cardioprotection the "first window" and "second window", respectively, which are now known as "early phase (or classical)" and "late phase" preconditioning. Subsequent studies revealed that the late phase of cardioprotection can persist for up to 72 h after preconditioning [13]. Thereafter, the major focus of studies on ischemic preconditioning moved to investigation of the subcellular mechanisms, with the aim of obtaining methods for application to pharmacological preconditioning and for new clinical therapies to control acute myocardial infarction.

In fact, the "early phase" and "late phase" of ischemic preconditioning are reported to share some trigger mechanisms, although different mechanisms may be involved in

the mediation of cardioprotection; the early phase is dependent on reactions that occur very rapidly, such as activation of ion channels or phosphorylation of enzymes, whereas the late phase involves processes that require far longer to occur such as modulation of the genes regulating channel proteins, receptor proteins, enzymes, molecular chaperon proteins, or immune factors. Thus, these two types of cardioprotection seem to share certain triggers, mediators, and effectors despite differences in the timing of participation in each cascade.

4. Cellular mechanisms of early ischemic preconditioning

4.1. Adenosine and protein kinase C (PKC)

In 1991, a study by Liu et al. [14] was performed at the laboratory of Downey that opened the door to pharmacological protection. Liu et al. used a rabbit model to show that inhibition of the adenosine receptor by administration of 8-SPT prior to sustained ischemia was able to abolish the protective effect of ischemic preconditioning. This report suggested that adenosine was a strong candidate as an agent for pharmacological preconditioning and a trigger factor for ischemic preconditioning. Taken together with the facts that (1) the adenosine A_1 receptor is one of the typical G-protein-coupled receptors (GPCRs) that have seven transmembrane domains, and (2) the intracellular Ca^{2+} concentration rises soon after the onset of ischemia, it was hypothesized that the subsequent cardioprotective response to an adenosine A_1 receptor-derived stimulus is related to both G-protein signals and Ca^{2+}. Thereafter, Ytrehus et al. [15] found that inhibition of PKC abolishes the limitation of infarct size by pretreatment with adenosine or by ischemic preconditioning, suggesting that PKC plays a pivotal role in the cardioprotective effect of preconditioning. Because PKC can be activated by either ischemia or by extracellular stimuli such as catecholamines (α_1-adrenoceptor stimulation), lipopolysaccharide (LPS), and PMA [16,17], thus leading to cardioprotection [18], it has come to be recognized as a major mediator of ischemic preconditioning.

On the other hand, we have reported that transient Ca^{2+} overload prior to sustained ischemia also has the same

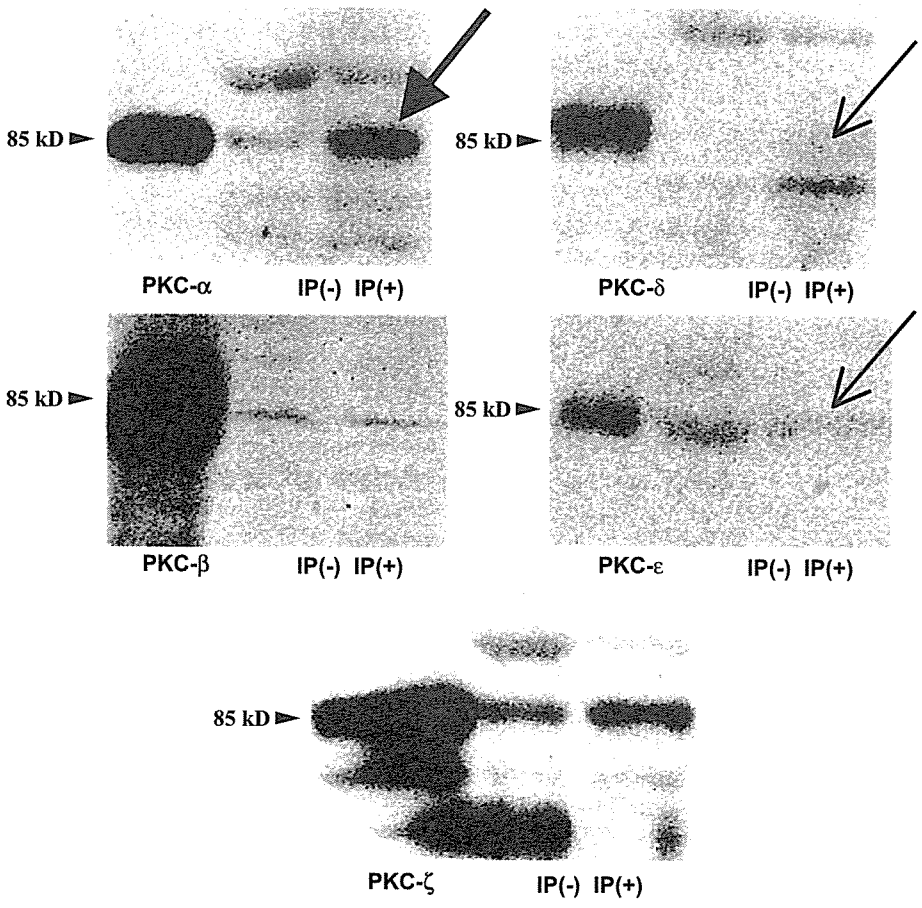

Fig. 1. Translocation of specific subtypes of PKC caused by ischemic preconditioning (IP) in anesthetized dogs. Myocardial samples were obtained after the completion of ischemic preconditioning. As shown in the figure, translocation of PKC-α was clearly increased after IP (bold arrow), while PKC-δ and PKC-ε showed no significant changes after IP (thin arrows), suggesting that PKC-α (but not PKC-δ or PKC-ε) plays a critical role in the triggering of IP in this in vivo canine model.

protective effect as ischemic preconditioning [17]. Furthermore, the cardioprotective effect of PKC is cancelled by GF109203X, a selective inhibitor of Ca^{2+}-dependent PKC (classical PKC) [19]. Because PKC-α is Ca^{2+}-dependent, these data suggest that triggering of the early phase preconditioning may be closely associated with transient changes of intracellular Ca^{2+} during a brief period of ischemia. While investigating the responsible subtype(s) of PKC in a dog model (Fig. 1) [20] and a rat model [21], we found that PKC-α mediates cardioprotection due to preconditioning in dogs, while other candidates such as PKC-δ [22–24] or PKC-ε [21,23–25] have been detected in smaller animals.

We have also studied the local metabolism of adenosine under normal and ischemic conditions [26]. Two enzymes [*S*-adenosylhomocysteine (SAH) hydrolase and 5′-nucleotidase] produce adenosine from SAH and AMP, respectively, while two other enzymes (adenosine deaminase and adenosine kinase) rapidly transform adenosine into inosine and AMP, respectively (Fig. 2). We have reported [19] that PKC directly activates ecto-5′-nucleotidase (5′-N; one of the endogenous adenosine-producing enzymes) which is located on the cell membrane. This enzyme maintains a low level of adenosine production under normal conditions but rapidly increases production as a specific response to ischemia or other extracellular stresses (which rapidly produces adenosine from AMP by its dephosphorylation in order to provide high-energy phosphates and to maintain the intracellular level of ATP) after phosphorylation of the serine/threonine residues of this enzyme. Because adenosine per se

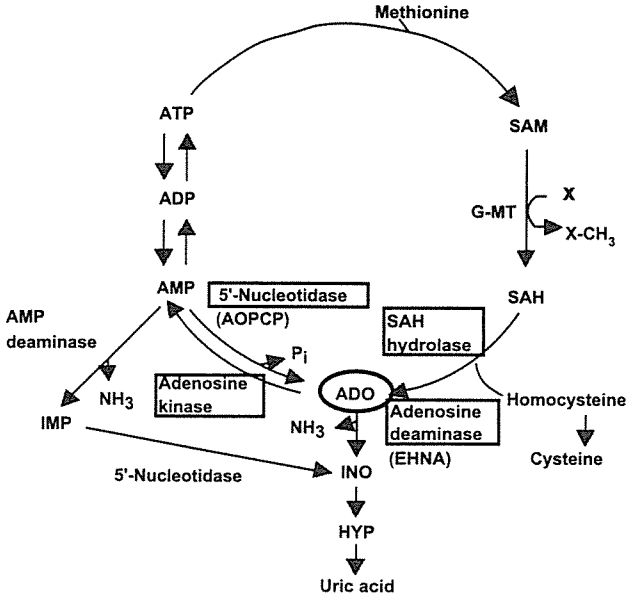

Fig. 2. Endogenous metabolic pathways of adenosine (ADO) and associated substances. Two enzymes [*S*-adenosylhomocysteine (SAH) hydrolase and 5′-nucleotidase] produce adenosine from SAH and AMP, respectively, while two other enzymes [adenosine deaminase (ADA) and adenosine kinase] rapidly transform adenosine into inosine and AMP, respectively. Specific pharmacological inhibitors of the respective enzymes are shown in parentheses.

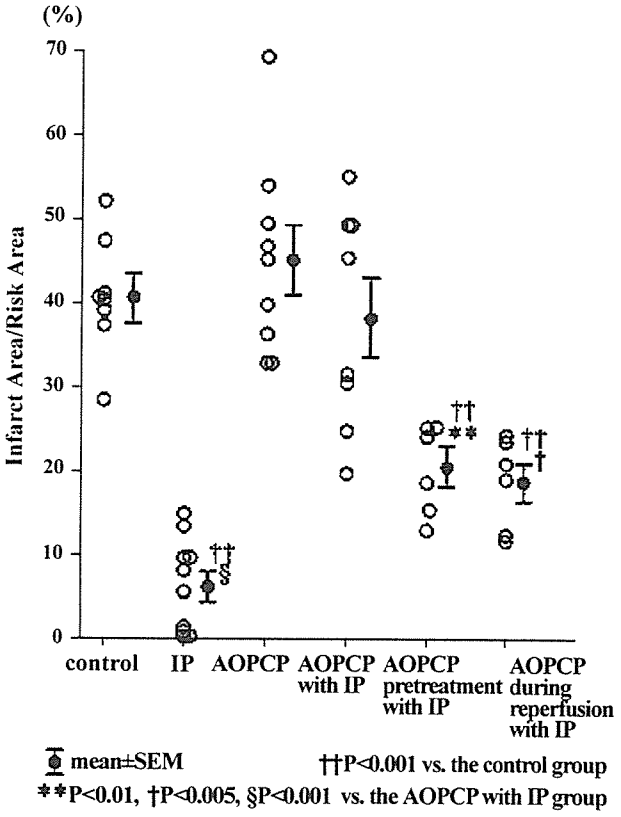

Fig. 3. Infarct size after 90 min of ischemia followed by 6 h of reperfusion in an anesthetized dog model. Abbreviations are shown in parentheses. Ischemic preconditioning (IP) markedly reduces infarct size, and this protection is blunted by administration of AO-PCP (a specific blocker of ecto-5′-nucleotidase) during either the preischemic or postischemic period.

is a bioactive endogenous modulator [27] with various effects on the cardiovascular system, including a negative inotropic effect, negative contractile effect, promotion of coronary blood flow, and antiplatelet activity, it could act as both a trigger and a mediator of ischemic preconditioning.

Although these findings could be seen as contradictory, by taking all the data together, it can be assumed that a circular pathway involving adenosine-PKC-ecto-5′-nucleotidase-adenosine may enhance the activation of other factors involved in cardioprotection due to ischemic preconditioning. In support of this, we have found that treatment of dogs with a specific ecto-5′-nucleotidase inhibitor (AOP-CP) during either preconditioning or early reperfusion can equally diminish the cardioprotective effect of ischemic preconditioning (Fig. 3) [28].

4.2. ATP-sensitive potassium channels (KATP channels)

Investigation of ATP-sensitive potassium channels (KATP channels) has a longer history than studies on ischemic preconditioning, since Noma [29] first reported the existence of these channels in the myocardium in 1983.

The KATP channel is an octamer (four Kir family subunits and four SUR subunits) that exists in the membrane

and is modulated by Mg and ATP [30]. KATP channels were first identified by cardiovascular physiology studies as causing vascular smooth muscle relaxation in either large or small arteries or as having a negative inotropic effect on cardiac myocytes [31].

Because KATP channels act as an inward rectifier [30] when activated, these effects could be caused by an increase of the depolarization threshold that reduces excitation of either vascular smooth muscle or cardiac myocytes followed by vasodilation and shortening of the action potential duration, respectively, which finally result in intracellular Ca^{2+} unloading [30,31] and reduced metabolic demand. These phenomena resemble the acute cardiac responses and cardioprotection afforded by ischemic preconditioning, so it has been hypothesized that KATP channels might be one of the critical effectors of either ischemic or pharmacological preconditioning [32]. Pharmacological preconditioning with KATP channel openers was first demonstrated in 1992 [33], and it was thought to be mediated intervention downstream of the A1 adenosine receptor [34].

In 1991, Inoue et al. [35] found that not only the cell membrane but also the inner mitochondrial membrane possessed ATP-sensitive inward rectifier activity, and they suggested the existence of "mitochondrial KATP channels" in contrast to "sarcolemmal KATP channels". Thereafter, the contribution of mitochondrial and sarcolemmal KATP channels to cardioprotection after ischemic preconditioning was studied extensively. Both Ca^{2+} unloading and preservation of ATP, which had been considered to be related to sarcolemmal KATP channels, were found to be actually mediated by mitochondrial KATP channels [36]. However, numerous studies on the cardioprotective effect of mitochondrial KATP channels have subsequently been performed, leading to some critical problems with the assumption that the KATP channels are the final effector of ischemic preconditioning. Firstly, "mitochondrial KATP channels" have still not been cloned after more than 10 years of investigation in spite of dramatic progress in the cloning of many mitochondrial proteins. It is now thought that mitochondrial KATP channels might not include the Kir 6.1 or Kir 6.2 subunits, which are common to sarcolemmal and other KATP channels [37], but their structure is largely unknown. Secondly, although some in vitro studies have shown a potent effect of putative modulators of mitochondrial KATP channels [38] (diazoxide as an opener of KATP channels and 5-hydroxydecanoate (5-HD) as an inhibitor which are almost the only tools available to test the function of these channels), both drugs also have other important direct effects on cellular respiratory metabolism. For example, diazoxide can reduce oxidative damage by a direct action on succinate dehydrogenase (SDH), and it modulates mitochondrial ATPase to preserve mitochondrial ATP [39], while 5-HD acts as a competitive inhibitor of acyl-CoA (a major substrate of the TCA cycle [40]) to antagonize diazoxide-induced changes [39]. Thirdly, some recent studies using other models have failed to show complete modulation of the cardioprotective effect of ischemic preconditioning by these two drugs [41,42]. Fourthly, Pain et al. [43] have reported that reactive oxygen species (ROS), which are transiently generated by opening of the mitochondrial KATP channels, activate downstream cascades that confer cardioprotection. In addition, a study on Kir 6.1 or Kir 6.2 knockout mice showed that mitochondrial KATP channel activity does not contribute to in vivo cardioprotection by ischemic preconditioning [37]. It is not clear why these differences exist, but some investigators focusing on mitochondrial KATP channels have suggested that the contribution of sarcolemmal KATP channels to cardioprotection may be more important in the beating hearts and less important under nonbeating experimental conditions (i.e., in vitro).

The most recent attempts to overcome this controversy have been studies directed towards the detection of components located on mitochondrial membrane that are also associated with SDH, based on the abovementioned finding that diazoxide and 5-HD can modulate either membrane KATP channel activity or mitochondrial SDH. In addition, more potent agents for activating mitochondrial KATP channels have been developed such as BMS191095 [44]. Although these ongoing studies are providing some possible features or characteristics of mitochondrial KATP channels, the actual cardioprotective role of these channels needs to be investigated further.

4.3. p38MAPK or PI3-K and their downstream cascades

The role of mitogen-activated protein kinases (MAPKs), which form part of the second messenger systems that mediate extracellular stimuli, in the cardioprotective effect of ischemic preconditioning has also been studied.

In 1997, Weinbrenner et al. [45] reported that ischemic preconditioning caused an increase of p38MAPK activation during sustained ischemia in rabbits which was correlated with the cardioprotection provided by preconditioning. However, p38MAPK was not activated during ischemia in the control group, while contradictory results were obtained in 1999 by in vivo [46] and in vitro [47] studies that suggested p38MAPK activation could promote ischemic damage. Interestingly, the latter study revealed that continuous hypoxia caused biphasic activation of p38MAPK in rat cardiomyocytes, with a transient peak occurring within 30 min and being followed by continuous activation after 4 h [47]. Treatment with anisomycin, a potent p38MAPK (and JNK) activator, just before ischemia could attenuate ischemic injury, with only the first peak of p38MAPK activation persisting and the second being abolished. This observation led us to hypothesize that p38MAPK activation has opposing effects; that is, transient activation prevents ischemic injury, while continuous activation exacerbates it. We found that repetitive short period(s) of ischemia and reperfusion cause transient but strong activation of p38MAPK, while, conversely, p38MAPK activation is attenuated during sustained ischemia (Fig. 4) [48].

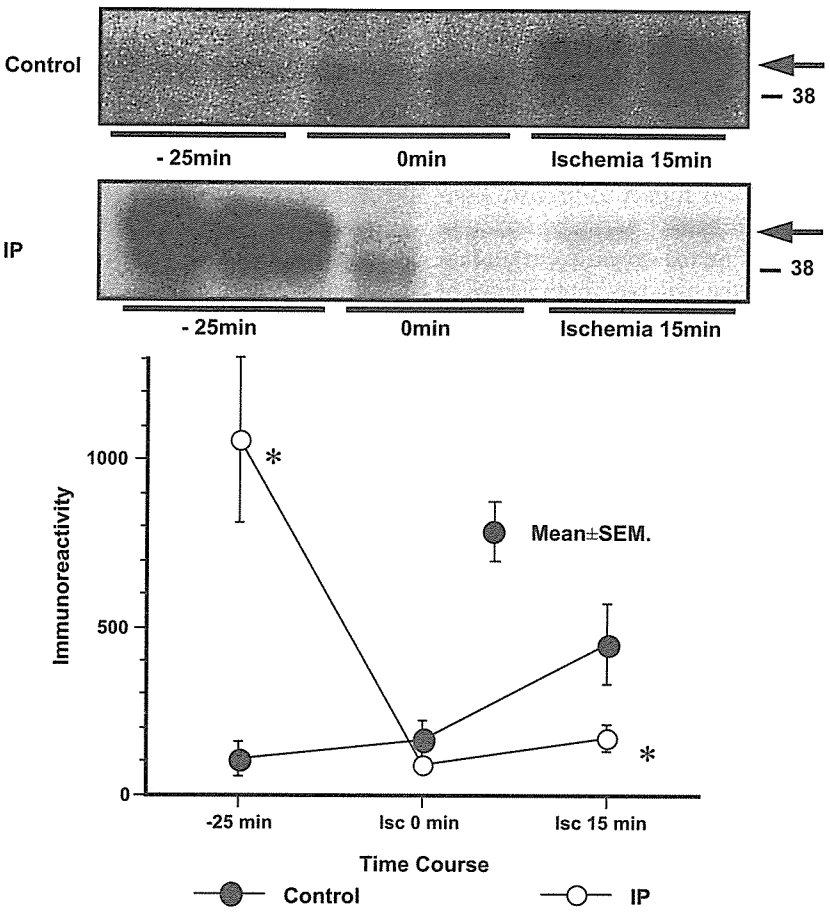

Fig. 4. p38MAPK activity estimated by the ratio of phosphorylated and total protein. Immunoblotting of the representative specimens (top) and the changes in mean value (bottom, n=3 or 4 each) are demonstrated. *P<0.05 vs control.

p38MAPK activation is known to activate the cell membrane glucose transporter (GLUT-4) and promote glucose uptake [49], whereas the expression of this transporter is regulated by phosphatidylinositol 3-kinase (PI3-K) [49] or 5′-AMP activated kinase (AMPK; published in abstract of Ref. [112]). Furthermore, MAPKAPK-2 and HSP27 (one of the small heat shock proteins that acts as a molecular chaperone), which are downstream of p38MAPK, are activated in preconditioned myocardium at the onset of sustained ischemia. Interestingly, MAPKAPK-2 subsequently activates Akt, which lies downstream of PI3-K [50], to antagonize apoptotic signals. PI3-K can be activated by IP [51] and is also reported to cause an increase of nitric oxide (NO) production and the downstream activation of PKC [51]. On the other hand, HSP27 binds to the z-bands of myofibrils to prevent ischemic degradation of myofilaments [52] or prevents the interaction of Apaf-1 with procaspase-9 through binding with cytochrome c [53] which is released from the mitochondria and enhances this interaction [54]. Both of these actions can ameliorate or delay ischemic cell death. A study of HSP27-overexpressing cells indicated that HSP27 might be able to protect the myocardium against ischemia [55], supporting this hypothesis. p38MAPK activation requires dual phosphorylation of its 180T-X-Y182 site, but the mechanism by which ischemia transiently activates p38MAPK is unclear. Some reports have suggested that both PKC [43,54] and some tyrosine kinases [24] may play a role, but we found that tyrosine kinase activation was unrelated to cardioprotection in dogs [56], at least with regard to the early phase of ischemic preconditioning. This issue should be investigated further.

4.4. Bradykinin and opioids

Some reports have suggested that bradykinin [57] may be a candidate trigger for preconditioning. The cardioprotective effect of bradykinin has been intensively investigated [58], and it is known that preconditioned hearts show an increase of the interstitial bradykinin level [59], while overexpression of kallikrein has a protective effect against ischemia [60]. The downstream effectors are reported to be an increase of nitric oxide production [61] or opening of

KATP channels [62] after activation of the bradykinin B_2 receptor [61–63].

While bradykinin is considered to be an endogenous trigger of preconditioning, as mentioned above, activation of the δ-opioid receptor by opioid peptides has also been investigated as a potent exogenous trigger of preconditioning in isolated human cardiac tissue [64]. Many reports have suggested that KATP channels are the downstream mechanism of cardioprotection, but the relative contribution of either sarcolemmal [65] or mitochondrial [62] KATP channels to the triggering phase is still controversial.

4.5. Other emerging factors

In addition, some of the cell membrane ion exchangers are also possible candidates for the mediation of cardioprotection due to preconditioning such as the Na^+/H^+ exchanger (NHE) [66], Na^+/Ca^{2+} exchanger (NCX), and Na^+/K^+ ATPase [67]. Because these channels contribute directly to ischemia/reperfusion injury, they have been studied as components of the cardioprotection afforded by ischemic preconditioning. However, the latest studies have positioned them as pharmacological therapeutic targets separately from their effect on preconditioning.

One of the emerging concepts is the involvement of the mitochondrial transition pore (MTP) which interacts directly with the activated PKC-ε isoform and inhibits calcium-induced pore opening to decrease mitochondrial permeability [68] or decrease mitochondrial release of cytochrome *c* in response to various stresses. On the other hand, recent studies have proposed a role of Bcl-2, an antiapoptotic protein that is also induced by ischemic preconditioning, in ischemic metabolic changes of the mitochondria through association with components of the respiratory chain.

Furthermore, Lochner et al. [69] reported that transient β-adrenoceptor stimulation mimics preconditioning independently of PKC, while we have found that activation of protein kinase A and subsequent transient p38MAPK activation confers a similar cardioprotective effect in dogs [70] (Fig. 5). The molecular mechanism of this PKA-induced transient activation of p38MAPK, which may help to explain how p38MAPK is transiently activated, may be that PKA phosphorylates the catalytic site of protein tyrosine phosphatase and inhibits dephosphorylation of p38MAPK, which leads to physiological augmentation of p38MAPK activity independently of PKC [71,72]. In addition, we observed in an in vivo dog model that Rho and Rho-kinase play an important role downstream of PKA during sustained ischemia to confer cardioprotection of ischemic preconditioning independent of PKC (published in abstract of Ref. [113]). These findings might also be useful with regard to clinical application because widely used drugs can elicit this effect without a negative inotropic effect even in acute heart failure. Taken together with the cardioprotection induced by α_1-adrenoceptor stimulation that we described previously, it seems possible that both the α_1-PKC pathway and the β-PKA pathway may "independently but synergistically" mediate catecholamine-induced preconditioning in response

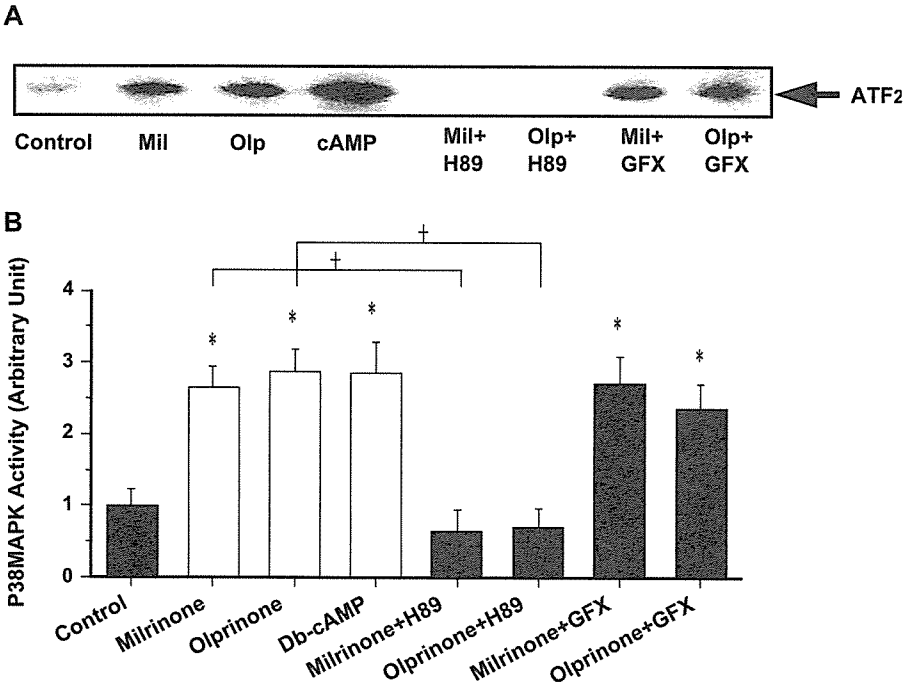

Fig. 5. p38MAPK activity in an anesthetized dog model (estimated by the phosphorylation of its substrate). Myocardial samples were obtained after 30 min of drug infusion. (A) Representative immunoblot specimens and (B) changes of the mean value (mean ± S.E.M.). Transient stimulation by cyclic AMP caused activation of p38MAPK which was blocked by a PKA inhibitor but not by a PKC inhibitor, suggesting that PKA can activate p38MAPK independent of PKC. Bars show the mean values ($n=4$). Mil: milrinone; Olp: olprinone; GFX: GF109203X. $^{\dagger}P<0.05$; $^{*}P<0.05$ vs. control.